

DOE/ID/12779-3
(DE95002658)
Distribution Category UC-1418

DEVELOPMENT OF NOVEL ACTIVE TRANSPORT
MEMBRANE DEVICES

Interim Report

By

Daniel V. Laciak

November 1994

Work Performed Under Contract No. DE-FC36-89ID12779

Prepared for the
U.S. Department of Energy
Under DOE Idaho Operations Office
Sponsored by the Office of the Assistant Secretary
for Energy Efficiency and Renewable Energy
Office of Industrial Technologies
Washington, D.C.

Prepared by
Air Products and Chemicals, Inc.
Allentown, PA

DISCLAIMER

**Portions of this document may be illegible
in electronic image products. Images are
produced from the best available original
document.**

Foreword

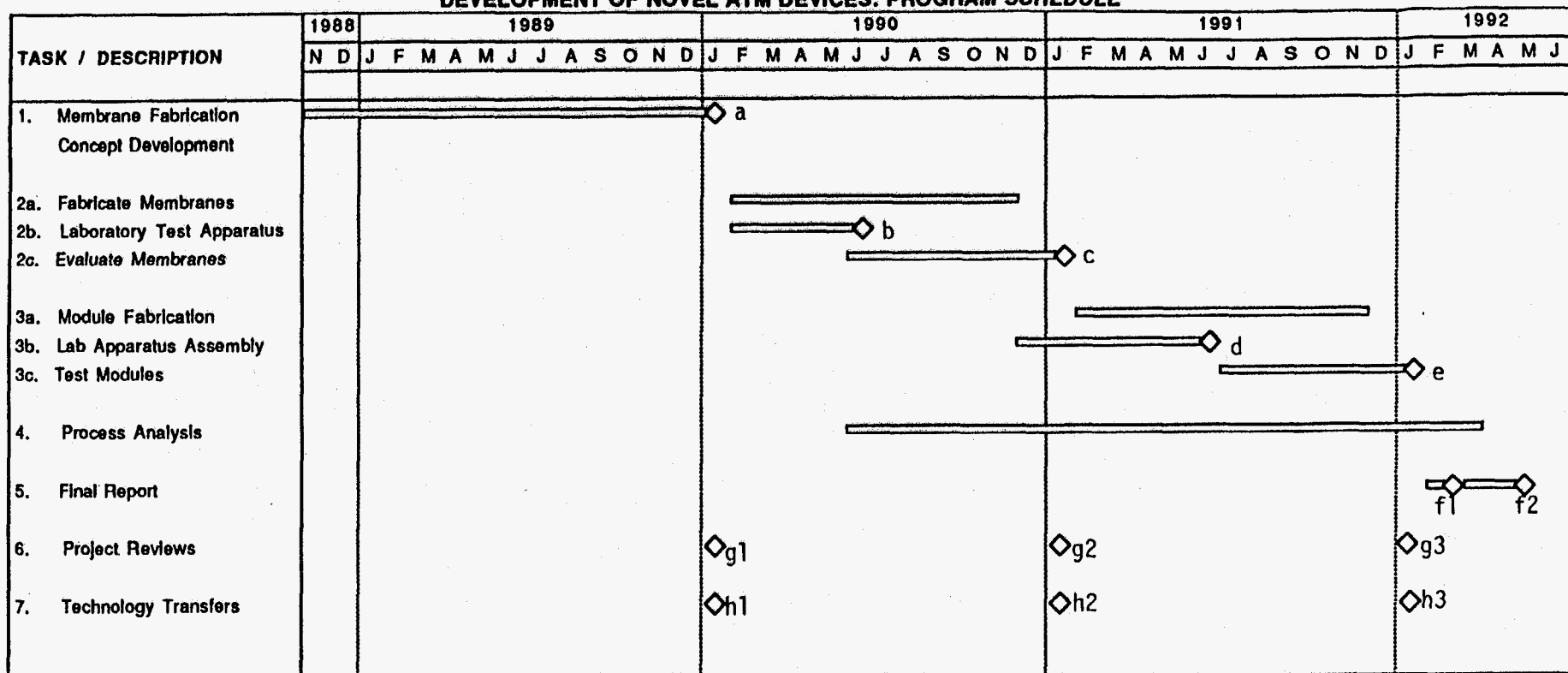
This interim report, prepared by Air Products and Chemicals, Inc., describes work performed during the second budget period of Cooperative Agreement NO. DE-FC36-89ID12779. The program was administered by the U.S. Department of Energy's Idaho Operations Office, Idaho Falls, Idaho. The Project Manager was Mr. David M. Blanchfield. Technical guidance was provided by Dr. Thomas Lawford of EG&G Idaho, Inc.

Air Products has undertaken a research program to fabricate and evaluate gas separation membranes based upon promising "active-transport" (AT) materials recently developed in our laboratories. Active Transport materials are ionic polymers and molten salts which undergo reversible interaction or reaction with ammonia and carbon dioxide. The materials are useful for separating these gases from mixtures with hydrogen. Moreover, AT membranes have the unique property of possessing high permeability towards ammonia and carbon dioxide but low permeability towards hydrogen and can thus be used to permeate these components from a gas stream while retaining hydrogen at high pressure.

The program was divided into three major tasks, each approximately one year in duration. The work plan/milestone chart for the 43-month contract period, which includes a 3-month no cost extension, is shown in Figure i. In the first task, various fabrication concepts were screened for feasibility. In the second task, the most promising fabrication concept, multilayer composite membranes, was evaluated under conditions typical of the target applications. In the third task, prototype, lab-scale modules will be fabricated and evaluated. Finally, data obtained during performance of Tasks 2 and 3, along with a market analysis (Task 4), will be used to perform an economic evaluation of the AT membrane-based separation process.

This report summarizes technical progress made during the second budget period. Detailed event scheduling, which incorporates the recommendations made at the end of the first budget period, is shown in Figure ii. Specific work proposed and completed under this program included:

DEVELOPMENT OF NOVEL ATM DEVICES: PROGRAM SCHEDULE



- a. Interim Report
- b. Complete Test Unit
- c. Complete Preliminary Tests
- d. Module Test Plan
- e. Complete Module Tests
- f1. Draft
- f2. Final
- g. Review Date
- h. At least one activity per year

Figure I

- Completion of microencapsulation feasibility study
- Completion of CO₂-selective MLC feasibility study
- Upgrade of membrane test equipment to accommodate high pressures
- Evaluation of MLC membranes at high pressures

This report concludes with an assessment of the program status and recommendations for further work.

Figure II: DEVELOPMENT OF NOVEL ATM DEVICES - YEAR 2

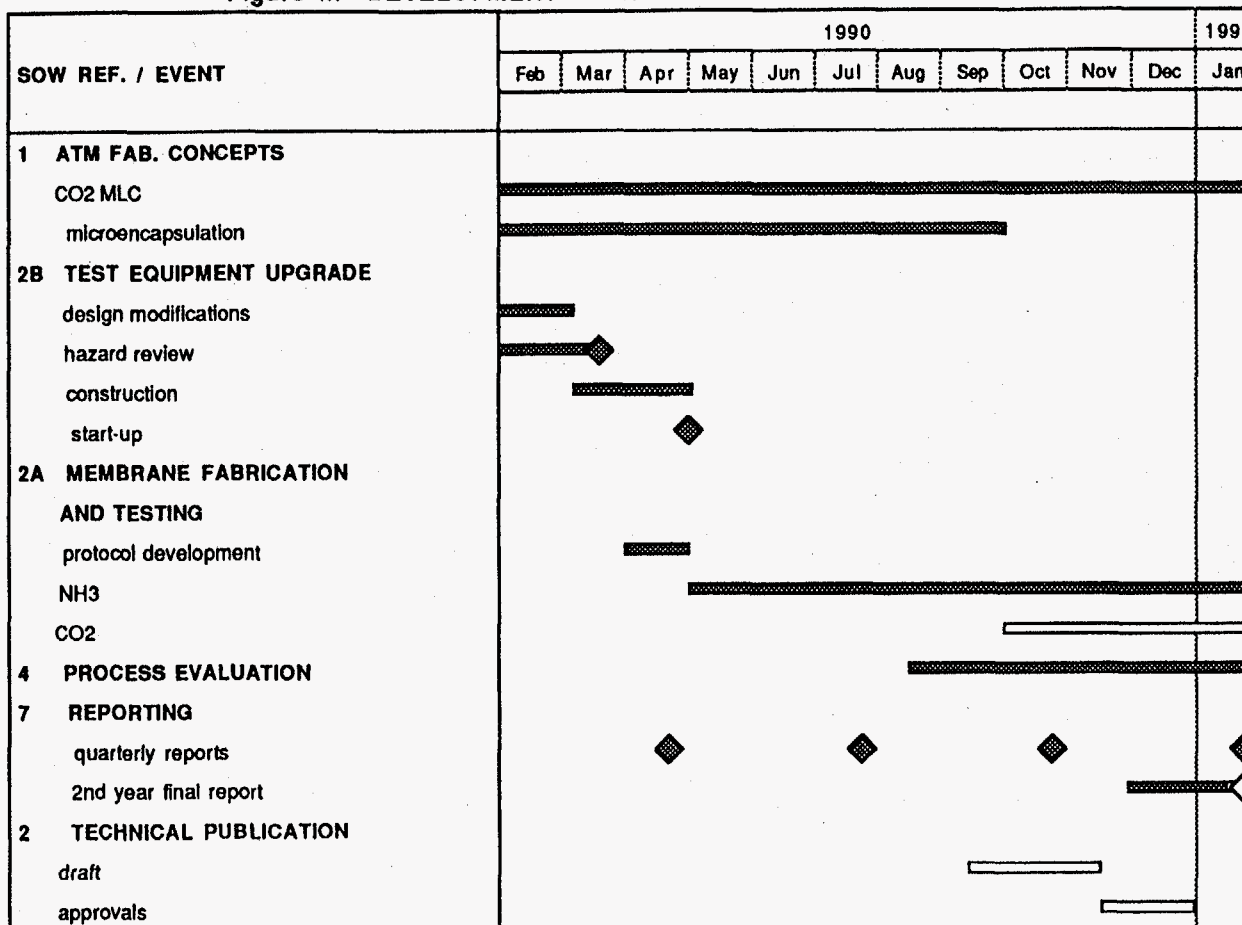


Table of Contents

1.0	Executive Summary	1
2.0	Microencapsulation of Active Transport Materials	3
3.0	Fabrication and Evaluation of CO ₂ -Selective MLC Membranes	26
4.0	Evaluation of NH ₃ -Selective MLC Membranes	44
5.0	Conclusions and Recommendations	75
6.0	References.....	78
7.0	Appendix-Summary of NH ₃ -Selective MLC Test Runs.....	79

List of Figures

Figure 2.1-1	SEM of PTMSP-encapsulated NH ₄ SCN Prepared via LCED - acetone collection (8-761)	18
Figure 2.1-2	SEM of PTMSP-encapsulated NH ₄ SCN Prepared via LCED - silicone oil collection (8-858)	19
Figure 2.1-3	SEM of PTMSP-encapsulated PVAmSCN Prepared via LRD - starch collection (8-711)	20
Figure 2.1-4	SEM of PTMSP-encapsulated NH ₄ SCN Prepared via LRD - acetone collection (8-711)	21
Figure 2.1-5	SEM of PTMSP-encapsulated TEAA•4H ₂ O Prepared via LRD Techniques -silicone (8-909, 8-911)	22
Figure 2.1-6	SEM of PTMSP-encapsulated TEAA•4H ₂ O Prepared via Solvent Extraction Techniques	23
Figure 2.1-7	SEM of PTMSP-encapsulated NH ₄ SCN Prepared via Phase Separation Techniques	24
Figure 2.1-8	SEM of PTMSP-encapsulated TEAA•4H ₂ O Prepared via Phase Separation Techniques	25
Figure 3.1-1	SEM of PTMSP/DADMAF/PTMSP MLC (11273-75)	40
Figure 3.1-2	SEM of PDMS/DADMAF/PDMS MLC (11638-50)	41
Figure 3.1-3	SEM of PDMS/DADMAF/PDMS MLC after Testing (11638-50)	42
Figure 3.1-4	SEM of PDMS/DADMAF/PDMS/DADMAF/PDMS 5-layer MLC (11638-102-1)	43
Figure 3.2-1	CO ₂ Permeance of PDMS/DADMAF/PDMS MLC (11638-50)	34
Figure 4.1-1	Debottlenecking/Hybrid Scenario Applied to Ammonia Synthesis	45
Figure 4.1-2	Total Ammonia Recovery from Ammonia Synthesis via Membranes	48
Figure 4.1-3	Relationship of Dew Point to Pressure for High Purity Ammonia Streams	49
Figure 4.2-1	Process Flow Diagram-High Pressure Membrane Test System	53
Figure 4.2-2	CYL-2 Connection Assembly-Expanded View	54
Figure 4.2-3	High Pressure Membrane Test Unit	55
Figure 4.2-4	Electrical Wiring Diagram-High Pressure Membrane Test System	56
Figure 4.2-5	Control Cabinet-High Pressure Membrane Test Unit	59
Figure 4.3-1	Evaluation of MLC Membrane as a Function of Feed Pressure	62
Figure 4.3-2	NH ₃ /H ₂ Selectivity of PTMSP/PVAmSCN/PAN/HT MLC Membrane	63
Figure 4.3-3	SEM of MLC Before and After Permeation Testing (11497-73)	65

List of Figures (continued)

Figure 4.3-4	Evaluation of PTMSP/PVAmSCN/PTMSP MLC Membrane	66
Figure 4.3-5	Concentration Polarization Phenomenon	68
Figure 4.3-6	Effect of Feed Flow Rate on Membrane Performance	69
Figure 4.3-7	Effect of Test Cell Geometry on Membrane Performance	72
Figure 5.3-1	Third Year Planning	77

List of Tables

Table 2.1-1	Centrifugal Coextrusion Microcapsules	5
Table 2.1-2	Rotating Disk Microcapsules	8
Table 2.1-3	Solvent Evaporation Encapsulation of TEAA•4H ₂ O	9
Table 2.1-4	Phase Separation Encapsulation	10
Table 2.2-1	Absorption Capacity of Microencapsulated AT Materials	12
Table 2.2-2	Absorption Capacity of PTMSP	14
Table 2.2-3	Least Squares Fit of Microencapsulation Data	15
Table 2.2-4	Selectivity of PTMSP-Encapsulated NH ₄ SCN and TEAA•4H ₂ O	15
Table 3.2-1	Evaluation of Free-standing DADMAF Membranes	28
Table 3.2-2	Evaluation of PTMSP/DADMAF/PTMSP MLC Membranes	30
Table 3.2-3	Evaluation of PTMSP/DADMAF/PTMSP MLC with SUR-1	31
Table 3.2-4	Evaluation of MEM213/DADMAF/MEM213 MLC Membranes	32
Table 3.2-5	Evaluation of PDMS/DADMAF/PDMS MLC Membranes	33
Table 3.2-6	Effect of Dew Point and Temperature on PDMS/DADMAF/PDMS MLC Membranes	34
Table 3.2-7	Effect of Gas Stream Hydration on Membrane Performance	35
Table 3.2-8	Evaluation of MLC Membranes with Improved Analytical System	36
Table 3.2-9	Investigation of Flaws and Defects	38
Table 3.2-10	Effect of Permeate Pressure on Membrane Performance	38
Table 4.1-1	NH ₃ Synthesis Converter Effluent Composition	47
Table 4.1-2	Membrane Test Plan and Target Membrane Performance	52
Table 4.3-1	Diffusion Coefficients for Ammonia	70
Table 4.3-2	Evaluation of MLC Membranes at Process Conditions	72

1.0 Executive Summary

Air Products and Chemicals, Inc., has discovered "active transport" materials which may be useful for separating ammonia and carbon dioxide from mixtures with other gases, especially hydrogen. These materials are molten salts and polyelectrolytes which are, respectively, liquids and gels under conditions specific to their process application. Traditional membrane fabrication techniques limit the utility of such membranes. Air Products, under this Cooperative Agreement, has investigated new ways to fabricate liquid and liquid-like materials into practical gas separation membranes and devices. These include microencapsulation and multilayer composite, or MLC, membrane fabrication.

Microencapsulation is a process whereby the active transport material is contained within a spherical shell of poly(trimethylsilylpropyne). During the course of this program ammonium thiocyanate and tetraethylammonium acetate tetrahydrate, active transport materials for ammonia and carbon dioxide respectively, were successfully encapsulated within poly(trimethylsilylpropyne). The capsules were shown to separate ammonia and carbon dioxide from nitrogen via pressure swing absorption, however, the size (100-500 μ m) and payload (50%) were not sufficient to pursue further fabrication into gas separation membranes. We believe that smaller, higher payload capsules are obtainable; however, based on promising results in other fabrication areas, no additional experimental work will be performed in this area.

MLC membranes consist of a thin film of an active transport polyelectrolyte which is contained or "sandwiched" between two films of a highly permeable but nonporous polymer such as silicone rubber or poly(trimethylsilylpropyne). The "encapsulating" polymer imparts mechanical stability to the membrane while offering minimal mass transfer resistance. MLC membranes containing carbon dioxide-selective active transport materials exhibited good permselectivity for carbon dioxide over hydrogen and showed no degradation during 3 weeks of continuous testing. MLC membranes incorporating ammonia-selective active transport polyelectrolytes were stable for up to 3 weeks of continuous testing at transmembrane pressures as high as 1900 psi. Concentration polarization effects were observed for these membranes at high feed pressures.

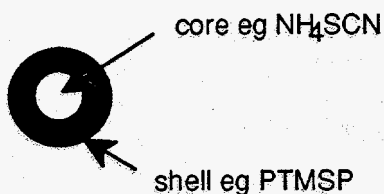
Based upon the promising results obtained thus far in this study, it is our recommendation to proceed with the fabrication of lab-scale membrane modules utilizing the multilayer composite

fabrication technique. Therefore, the major planned activities for the next segment of the program include:

- synthesis of active transport polyelectrolytes and MLC component polymers
- upgrade of membrane test unit to accommodate lab-scale modules
- identification of a module fabrication subcontractor
- evaluation of lab-scale modules under end-use conditions
- continued market survey/economic analysis of membrane-based separation schemes to recover ammonia from ammonia synthesis gas and carbon dioxide from steam reformers

2.0 Microencapsulation of Active Transport Materials

Microencapsulation is a process wherein one material is encased within another to form a small, usually spherical particle. An idealized microcapsule can be viewed as a core of "fill" material surrounded by a shell or "skin" as shown below.



Microencapsulation has been practiced commercially for at least 30 years. Many products including medications, flavors, and pesticides incorporate microcapsules. In all these examples microencapsulation serves one of two purposes: a) to increase the shelf-life of a reactive material by storing it in an impermeable shell, or b) to control the release and delivery of the core material through the shell. Our purpose for using microencapsulation is different. We wish to permanently "store" a material within the capsule while allowing gases to permeate, in both directions, through the shell. Our concept was to microencapsulate the AT material, that is, the gas-interactive component (e.g. NH₄SCN), within a shell of a nonporous but gas-permeable polymer such as poly(trimethylsilylpropyne) or silicone rubber. These capsules could then be utilized in gas absorption processes or fabricated into a gas separation membrane via immobilization within a microporous matrix or by imbedding them within a dense polymer matrix¹. Microencapsulation of the AT material was performed under a subcontract in the laboratories of Southwest Research Institute, San Antonio, Texas. Before fabrication into membranes was attempted, the samples were evaluated by two methods. The first was to perform scanning electron microscopy (SEM) on the "as received" samples in order to determine capsule size and general appearance. Particular attention was paid to detection of defects in the capsule wall. The second method was to measure their gas absorption capacity in order to obtain information on the activity of the AT component and the payload of the capsule. (The "payload" is defined as the weight percent AT component.) We have previously determined² that, to be useful in a membrane configuration, the capsule should a) be of the order of 1-50 μm in diameter, and 2) have a high payload (>85%) or absorption capacity combined with good selectivity over the inert gas.

2.1 Capsule Fabrication

The capsules were prepared by one or more of four microencapsulation techniques - rotating disk, centrifugal coextrusion and phase separation, and solvent evaporation. A general description of the encapsulation methods is given in a previous report³. The experimental parameters and other details relating to particular technologies used to microencapsulate TEAA·4H₂O. and NH₄SCN are given below and in Tables 2.1-1 through 2.1-4. Some of the data on PTMSP-encapsulated NH₄SCN, was reported previously⁴. This data is again presented here so that the study can be viewed as a whole.

2.1.1 Laboratory Centrifugal Extrusion Nozzle

The laboratory centrifugal coextrusion device, LCED, was used to prepare microcapsules containing ammonium thiocyanate. This device consists of a head with two nozzles and a concentric feed tube which is sealed to the head through a seal arrangement. For these feasibility experiments, this device was used with one nozzle plugged. The head was attached to a rotating shaft such that the direction of rotation was around its long axis. The shell material was fed by a Zenith®, gear pump through the feed tube into the head. The core was fed with a Zenith®, pump for runs 1-1 through 1-6. For the other runs, the gear pump was replaced by a syringe pump to minimize contamination of the feed solution. As the head rotated, the shell solution flowed through the outer orifices while the core material flowed through the inner orifice of the nozzle, creating a rod of fill material surrounded by a sheath of the shell solution. The centrifugal force from the rotating head broke the extruded rod into individual droplets (capsules) which were collected in an appropriate extraction bath. The size of the capsules was controlled by head speed, feed rate, and nozzle size.

Thirteen encapsulation runs were conducted using the LCED. Table 2.1-1 describes the details of the these runs. For the first seven, an acetone bath was used to collect the microcapsules. The capsules were removed from the bath and dried in air. During the drying process the outer film was observed to shrink and crack allowing some of the core to leak out (Figure 2.1-1). The evaluation of these initial runs indicated payloads (loadings) much lower than the theoretical payload (Table 2.2-1).

Table 2.1-1
Centrifugal Extrusion Microcapsules

Run # (Sample #)	Core Formulation	Shell Formulation	Theoretical Payload (%)	Sample Wt (grams)	Collection Bath	Comments
1-1	50% NH ₄ SCN 50% DI H ₂ O	2% PTMSP (med MW) 98% CHCl ₃	81	0	acetone	Shell was stringing at the nozzle. No capsules were made.
1-2 (8-761)	"	"	81	0.7	"	Sample formed OK. Some stringing. 5.9% loading
1-3 (8-762)	"	"	81	1.7	"	Capsules formed well. 5.7% loading
1-4 (8-763)	"	0.5% PTMSP (high MW) 99.5% CHCl ₃	92	trace	"	Capsules not formed well. Solution too viscous. 6.1% loading
1-5 (8-764)	"	3%PTMSP (med MW) 97% hexane	75	0.5	"	Capsules flattened on the surface of the acetone bath. 0% loading
1-6 (8-765)	"	2% PTMSP (med MW) 98% CHCl ₃	80	1.3	"	Capsules formed OK. Gear pump replaced with a syringe pump.
1-7 (8-857)	"	"	81	2	"	Some stringing. Capsules formed fairly well.
1-8	66.7% NH ₄ SCN 33.3% DI H ₂ O	5% PTMSP (low MW) 95% toluene	84	none	different oils	Different collection baths investigated. Lightweight silicone oil best.
1-9	31% NH ₄ SCN 69% methanol	"	71	none	different oils	Different collection baths investigated. Lightweight silicone oil best.

Table 2.1-1 (continued)
Centrifugal Extrusion Microcapsules

Run # (Sample #)	Core Formulation	Shell Formulation	Theoretical Payload (%)	Sample Wt (grams)	Collection Bath	Comments
1-10 (8-858)	66.7% NH ₄ SCN 33.3% DI H ₂ O	5% PTMSP 95% toluene	84	62	silicone oil (10 cst)	Sample placed in vacuum oven at 100°F. Capsules sieved out, rinsed with water and dried in air. 40% loading
1-11	31% NH ₄ SCN 69% methanol	"	71	none	"	Shell strings badly.
1-12 (8-859)	"	3.8% PTMSP (low MW) 96.2% toluene	71	37	"	Capsules flattened slightly on surface of silicone oil. Same drying procedure as above. 20% loading
1-13 (8-969)	66.7% NH ₄ SCN 33.3% DI H ₂ O	2% PTMSP (low MW) 98% toluene	83	18	"	Shell polymer concentration reduced to make smaller capsules. Capsules dried by heating in silicone oil to 140°F.

To prevent this problem, different collection baths were investigated including Isopar E, different grades of silicone oil, and water. The capsules tended to flatten on the surface of the water. Addition of a surfactant allowed the microcapsules to penetrate the water bath but the capsules coalesced, forming large agglomerates. A low viscosity (10 cst) silicone oil provided the best results. The capsules gradually harden leaving discrete particles (Figure 2.1-2). The solvent was gradually evaporated in a vacuum oven at 100°F or using a hot silicone bath (140°F) with agitation. The capsules were then sieved, rinsed with water, and dried in air.

Other runs examined the effect of increasing the concentration of NH₄SCN, using a methanol solution of NH₄SCN as the core, changing the solvent for the shell polymer, and varying the concentration of polymer in the shell formulation. Using methanol in the core solution should form an inner wall on the capsules to give more integrity to the coating as it dries. The use of

different solvents for the shell polymer affects the evaporation rate which varies the solidification rate. Lowering the shell polymer concentration decreases the viscosity of the solution and, in theory, allows for the formation of smaller capsules. None of these methods was particularly effective.

2.1.2 Laboratory Rotating Disk Device

The laboratory rotating disk device, LRD, consists of a high-speed, rotating disk which forms small, spherical droplets from an emulsion of the aqueous or solid salt in the shell polymer solution as it is fed onto the disk. The liquid droplets, which are formed at the periphery of the disk, are solidified by solvent evaporation. The size of the microspheres is controlled by the feed rate, disk speed and emulsion viscosity. The microspheres were collected in a thin layer of Dry-Flo®, starch, a solvent bath, or a silicone oil bath.

Table 2.1-2 summarizes the experimental parameters used on the samples prepared via the LRD. The first four samples were collected in Dry-Flo® starch to cushion their impact and maintain discrete, nonsticky particles; these capsules contained a gross excess of starch in the shell (Figure 2.1-3). Other samples were collected in acetone (Figure 2.1-4), methanol, or silicone oil. The samples collected in silicone oil (Figure 2.1-5) were made by recrystallizing TEAA•4H₂O in the shell polymer solution. For this process, the salt was dispersed in the shell solution, and the solution was then heated above the melting point of the salt (46°C) with stirring to form molten spheres of TEAA•4H₂O. For run 1-14 the solution, containing the molten salt, was poured onto the rotating disk. For runs 1-15 through 1-20 the solution was first cooled to room temperature to recrystallize the salt before it was poured onto the disk. Run 1-17 was rinsed in CH₂Cl₂ followed by acetone. Dichloromethane seemed to soften the wall which resulted in some agglomeration. Runs 1-18 through 1-20 were rinsed with acetone, water, and then acetone again.

Table 2.1-2
Rotating Disk Microcapsules

Run # (Sample #)	Core Formulation	Shell Formulation	Collection Medium	Disk Speed	Sample Wt (g)	Theoretical Payload (%)
1-1 (8-673)	2.5% PVAmSCN in DI H ₂ O	3% PTMSP (med MW) in hexane	starch	2030 rpm	1.5	30
1-2 (8-674)	"	2% PTMSP (med MW) in CHCl ₃	"	"	0.4	39
1-3 (8-675)	50% NH ₄ SCN in DI H ₂ O	3% PTMSP in hexane	"	"	5.5	90
1-4 (8-676)	50% NH ₄ SCN in DI H ₂ O	2% PTMSP (med MW) in CHCl ₃	"	"	2.5	94
1-5 (8-710)	2.5% PVAmSCN in DI H ₂ O	"	methanol	900	0.4	39
1-6 (8-711)	2.5% PVAmSCN in DI H ₂ O	"	acetone	"	0.2	38.5
1-14	TEAA·4H ₂ O	2% PTMSP (med MW) Isopar E	silicone oil (10 cst)	300	not collected	90
1-15 (8-970)	"	"	"	200	15.6	"
1-16	"	2% PTMSP (high MW) Isopar E	"	360	not collected	"
1-17 (9-155)	"	"	"	1032	0.1	"
1-18 (9-156)	"	2% PTMSP (low MW) Isopar E	"	280	0.3	"
1-19 (9-157)	"	"	"	1000	0.4	"
1-20 (9-158)	"	"	"	318	5.4	95

2.1.3 Solvent Evaporation

In the solvent evaporation method, the salt is dispersed in the carrier solvent (triacetin) or the shell polymer solution. The TEAA·4H₂O was recrystallized as described in section 2.1.2. The shell polymer was then added, with agitation, to the carrier solvent. Because the carrier solvent is immiscible with the shell polymer solution, a layer of the shell solution surrounded the dispersed salt droplets. Table 2.3-1 describes the various solvent evaporation samples prepared for this project. These capsules tended to coalesce during harvesting (Figure 2.1-6).

Table 2.1-3
Solvent Evaporation Encapsulation Of TEAA·4H₂O

Run # (Sample #)	Shell Polymer Formulation	Theoretical Payload (%)	Comments
1-5 (8-913)	2% PTMSP (low MW) 98% hexane	90	The salt was melted in the carrier solvent and agitated to form molten droplets. The solution was cooled to solidify the droplets. The polymer solution was added and the mixture was stirred for 7 hrs to evaporate the hexane.
1-6 (8-966)	"	"	This sample was a repeat of 8-913. TEAA was recrystallized in triacetin. Polymer solution was added to the salt/triacetin dispersion. The product was rinsed with acetone after filtration.
1-8 (8-967)	2% PTMSP (low MW) 98% Isopar E	"	The salt was recrystallized in the polymer solution to make smaller capsules. The salt/polymer dispersion was then dispersed in the triacetin carrier. The system was agitated to evaporate the Isopar and then filtered and rinsed in acetone.
1-9 (9-159)	"	95	"

2.1.4 Phase Separation

The phase separation technique involves dispersing the salt into the shell polymer solution. Then a phase separation initiator, a material which is miscible with the shell polymer solvent but one in which the shell polymer is insoluble, is added dropwise to the dispersion to cause the polymer to precipitate from solution and onto the dispersed phase. The product was then filtered out of the solvent and dried. Table 2.1-4 contains details on the samples prepared by phase separation methods. This method worked best on NH₄SCN. As shown in Figure 2.1-7, capsules of 25-50 μ m diameter were made, but they agglomerated into larger particles and could not be further separated.

Table 2.1-4
Phase Separation Encapsulation

Run# (Sample #)	Shell Formulation	Theoretical Payload (%)	Initiator	Comments
1-1 (8-909)	3% PTMSP (low MW) 97% toluene	77	silicone oil (10cst)	The product was collected on a 45 μ m sieve and rinsed with water. Product was dried in a convection oven.
1-2 (8-910)	2% PTMSP (high MW) 98% hexane	85	ethyl acetate	When the agitation was stopped, the water layer separated out. It is believed that some of the product is free polymer, not encapsulated salt. This may have been because the ethyl acetate was added too quickly.
1-3 (8-911)	"	"	"	Ethyl acetate added slower using a separatory funnel. Some improvement in the product.
1-4 (8-912)	2% PTMSP (high MW) 98% toluene	"	isopropanol	Isopropanol seemed to work better than ethyl acetate. Discrete capsules were observed in the liquid. During the drying process, the capsules appeared to collapse and stick together.
1-7 (8-968)	2% PTMSP (low MW) 98% Isopar E	90	silicone oil (10cst)	TEAA•4H ₂ O dispersed in the polymer solution. Salt was recrystallized by heating and then cooling the solution. Polymer was phased out of solution using silicone oil.

2.2. Capsule Evaluation

2.2.1 Gas Absorption Capacity

The gas absorption capacity of the capsules was measured using standard volumetric techniques. A dosing volume of gas was expanded into a reactor containing the sample, which was previously evacuated, and then allowed to reach equilibrium. The amount of gas absorbed was calculated from the known volumes, temperatures, and pressures. Results are reported in Table 2.2-1. (The different significant figures in the absorption capacity reflect improvements made in the sensitivity of the equipment during the course of this work.) The loading, or payload, was determined by dividing the NH₃ capacity of the capsule by the NH₃ capacity of the salt alone (as calculated from literature values) at the same temperature and pressure. The NH₃ capacity of most capsules was relatively poor. A few however, (e.g., 8-858, 8-911) had good NH₃ capacity and were chosen for further study. For the TEAA•4H₂O/PTMSP capsules, interpretation of the data is more complex. Here, capacity alone is not a good indicator of payload because PTMSP itself has a relatively high capacity for CO₂ (Table 2.2-2). In fact, payloads could not be calculated accurately for these systems using this method. In this case, the criterion for a well made TEAA•4H₂O capsule is the CO₂/N₂ selectivity of the capsule as compared to the CO₂/N₂ selectivity of PTMSP alone. This criteria was also applied to PTMSP-encapsulated NH₄SCN.

2.2.2 Selectivity

In order to determine the selectivity of the capsules, a N₂ absorption isotherm was measured at the same temperature as that obtained for the reactive gas (NH₃ or CO₂). In all cases N₂ absorption was found to be linear in pressure over 50-500kPa. A Henry's law constant was calculated from a linear least squares fit of the data (Table 2.2-3). The selectivity of the capsule was determined by calculating (from Table 2.2-3) the N₂ capacity of the capsule at a pressure for which the CO₂ or NH₃ capacity was determined experimentally (Table 2.3-1). Ammonia, CO₂, and N₂ absorption isotherms were then measured for PTMSP alone at the temperature of interest, and the Henry's law constants were determined as above. The selectivity of PTMSP was calculated at the same pressure as that used in the selectivity determination for the microcapsules. Results are shown in Tables 2.2-2 through 2.2-4. It can be seen that PTMSP-encapsulated TEAA•4H₂O is 4-9 times more selective than PTMSP alone (8-970, 8-967). Similarly, PTMSP-encapsulated NH₄SCN is roughly 17 times more selective than PTMSP. Thus, it is confirmed that the capsules do indeed contain an active component which imparts

Table 2.2-1
Absorption Capacity of Microencapsulated AT Materials

Sample ID	Sample #	Gas	T(°C)	P(kPa)	mmol/g	Loading
8-761	11163-29A	NH ₃	18	262 432 569	3.5 7.5 12.3	5.9%
8-762	11163-30A	NH ₃	17	391 564	5.7 10.9	5.7%
8-764	11163-29B	NH ₃	18	414 558	6.4 12.0	6.1%
8-765	11163-31A	NH ₃	18	389 597	0 0	0
8-857	11163-62B	NH ₃	20	252 615	2.4 10.0	4%
8-858	11163-60A	NH ₃	20	225 395	22.9 32.1	40%
	11163-63B	N ₂	20	221 404	0 0	
	11163-65B	NH ₃	20	215 397	20.77 43.7	50%
8.859	11163-61C	NH ₃	20	274 404	12.8 15.4	20%
8-909	11163-97	NH ₃	18	106 216 323 448 566	7.9 10.0 11.2 13.2 18.7	16%
8-910	11163-98	NH ₃	18	217 428 569	12.3 14.7 25.4	18%
8-911	11163-100	NH ₃	22	122 216 301 430	8.8 11.9 14.7 20.0	17%
	12008-14	N ₂	22	86 169 271 376	0.2670 0.0536 0.1047 0.1781	

Table 2.2-1 (continued)
Absorption Capacity of Microencapsulated AT Materials

Sample ID	Sample #	Gas	T(°C)	P(kPa)	mmol/g	Loading
8-912	11163-99	NH ₃	19	112	0	0
				211	0	
				330	0	
				435	0	
8-969	11497-5	NH ₃	21	222	0	0
				324	0	
				445	0	
				545	0	
8-913	11273-90	CO ₂	50	111	0.308	---
				267	0.510	
				476	0.772	
8-967	11674-27	CO ₂	50	55	0.531	---
				190	1.021	
				341	1.623	
				516	2.016	
		N ₂	50	104	0.006	
				198	0.011	
				291	0.016	
				378	0.021	
				460	0.028	
	11674-29	CO ₂	50	77	0.379	---
				156	0.658	
				241	1.098	
				256	2.588	
8-970	11638-93	CO ₂	50	140	0.224	---
				222	0.302	
				371	0.356	
				526	0.453	
		N ₂	50	68	0.002	
				121	0.003	
				220	0.007	
				465	0.017	

selectivity to the system. Also, since the loadings are at best only ~50%, the selectivity could be enhanced even further by increasing the payload.

Table 2.2-2
Absorption Capacity of PTMSP

<u>Sample #</u>	<u>Gas</u>	<u>T(°C)</u>	<u>P(kPa)</u>	<u>mmol/g</u>
12008-16	NH ₃	24	70	0.336
			178	0.909
			249	1.400
			301	1.845
			373	3.883
12008-12	N ₂	24	108	0.0528
			195	0.1002
			289	0.1524
			384	0.2038
			480	0.2636
12008-8	N ₂	50	81	0.276
			148	0.0495
			186	0.0640
			373	0.1361
			432	0.1557
11354-71A	CO ₂	50	120	0.4680
			289	1.089
			391	1.353
			502	1.728

Table 2.2-3
Least Squares Fit of Microcapsule Absorption Data

<u>Sample</u>	<u>Gas/T(°C)</u>	<u>K_H(mmol/g•kPa)</u>	<u>Intercept</u>	<u>R Value</u>
8-911	N ₂ /24	0.005238	-0.02735	0.9883
8-967	N ₂ /50	0.00005895	-0.000394	0.9968
8-970	N ₂ /50	0.00003718	-0.000699	0.9957
12008-16	NH ₃ /24	0.006027	-0.064019	0.9945
RQ193	CO ₂ /50	0.003417	0.037111	0.9982
12008-8	N ₂ /50	0.0003718	-0.00416	0.9997
12008-12	N ₂ /24	0.0005631	-0.009411	0.9997

Table 2.2-4
Selectivity of PTMSP-Encapsulated NH₄SCN and TEAA•4H₂O

<u>Gas Type</u>	<u>Sample id</u>	<u>Pressure (kPa)</u>	<u>Selectivity</u>
CO ₂ /N ₂	8-967	190	93
CO ₂ /N ₂	8-970	222	43
CO ₂ /N ₂	PTMSP	222	11
NH ₃ /N ₂	8-911	122	185
		216	131
		301	114
NH ₃ /N ₂	PTMSP	100	11.4
		200	11.1
		300	10.9

2.3 Summary/Status

Some general conclusions concerning microencapsulation of NH₄SCN and TEAA are summarized below.

NH₄SCN

Rotating Disk

- Capsule recovery/collection in Dry-Flo® starch is not a viable process. Too much starch becomes imbedded within the capsule wall. (Figure 2.1-3)
- Collection in a nonsolvent (eg acetone, methanol) improved the overall appearance of the capsules (Figure 2.1-4) but led to the formation of small defects in the shell which allowed the core to leak out. It is believed that this accounts for the low NH₃ absorption capacity of these capsules. (Table 2.2-1). Size ranged from 200-800 μ m diameter.

Centrifugal Coextrusion

- Acetone collection led to shell wall shrinkage and subsequently to cracks in the shell. As these capsules had lower than expected capacities, it seems reasonable that the core was lost through these cracks.
- Silicone or other oil baths gave best results. Capsules were defect-free and had improved NH₃ absorption capacity but tended to coalesce (Figure 2.1-2). Capsule diameter was >250 μ m.

Phase Separation

- Good capsule formation, but isolation of discrete particles was a problem. Capsules as small as 25-50 μ m were produced but agglomerated into larger (500 μ m) particles (Figure 2.1-7). Absorption properties were good.

TEAA·4H₂O

Rotating Disk

- The combination of a low volatility solvent for PTMSP (Isopar E) and a silicone oil collection bath gave well-defined, discrete capsules ca 500 in diameter (Figure 2.1-5). The shell was smooth and free of defects. This technique appears viable but capsule size needs to be reduced 10-fold to be implemented in a commercially attractive membrane.

Solvent Evaporation

- Triacetin acceptable as a carrier solvent. Capsules were largely defect-free but tended to coalesce (Figure 2.1-6). Absorption capacity suggests capsules have lower salt content than expected.

Phase Separation

- Good capsule formation although shell appears to contain an excess of free polymer on the surface (Figure 2.1-8). In view of the high CO₂ capacity of PTMSP, this may account for the higher than expected CO₂ capacity of these capsules.

Both NH₄SCN and TEAA·4H₂O have been encapsulated within PTMSP. In general, TEAA seems more amenable to microencapsulation because it can be melted and is thus easily processed by phase separation or solvent evaporation microencapsulation techniques. Thus far, capsules of the necessary size and payload combination, which would be amenable to further fabrication into a membrane device, have not been produced. Thus, such fabrication has not been attempted. Based on the positive gas absorption results, a patent for the use of microencapsulated AT materials as PSA, VSA, etc. absorbents is being actively pursued. Further work addressing a decrease in capsule size with a concurrent increase in loading would be necessary before attempting to fabricate a practical membrane device. No further work is anticipated under this cooperative agreement.

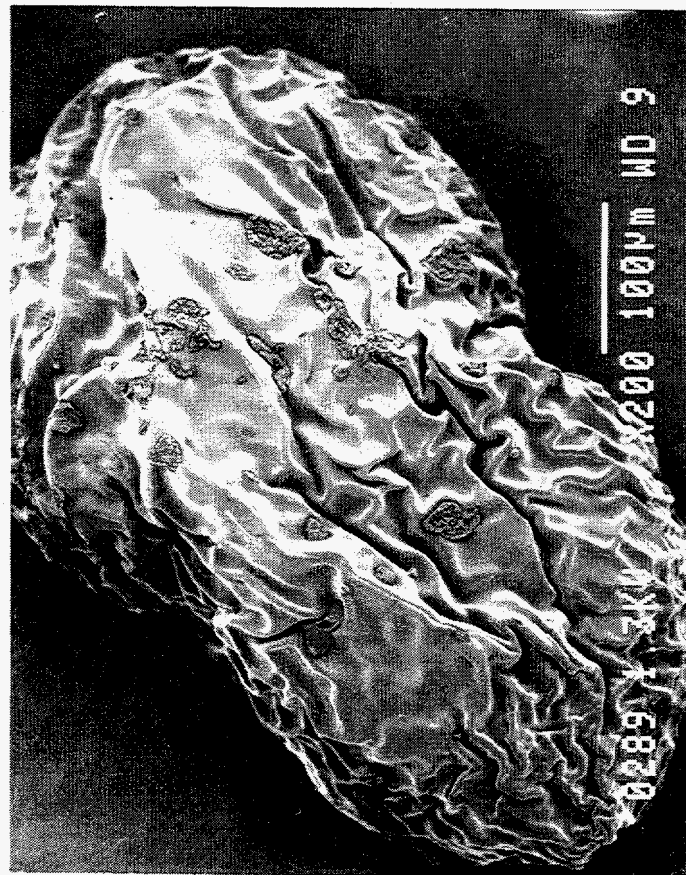
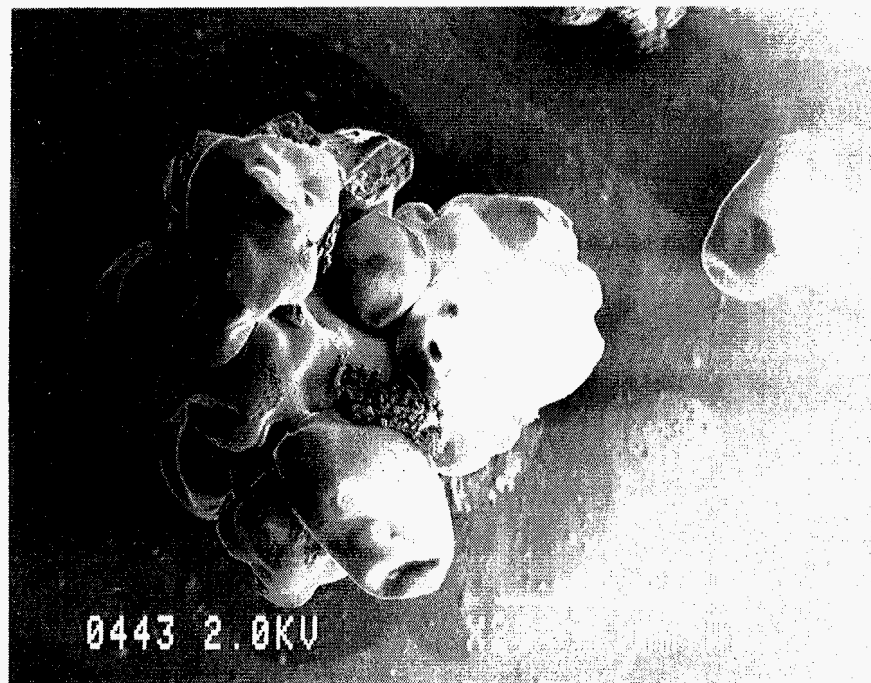


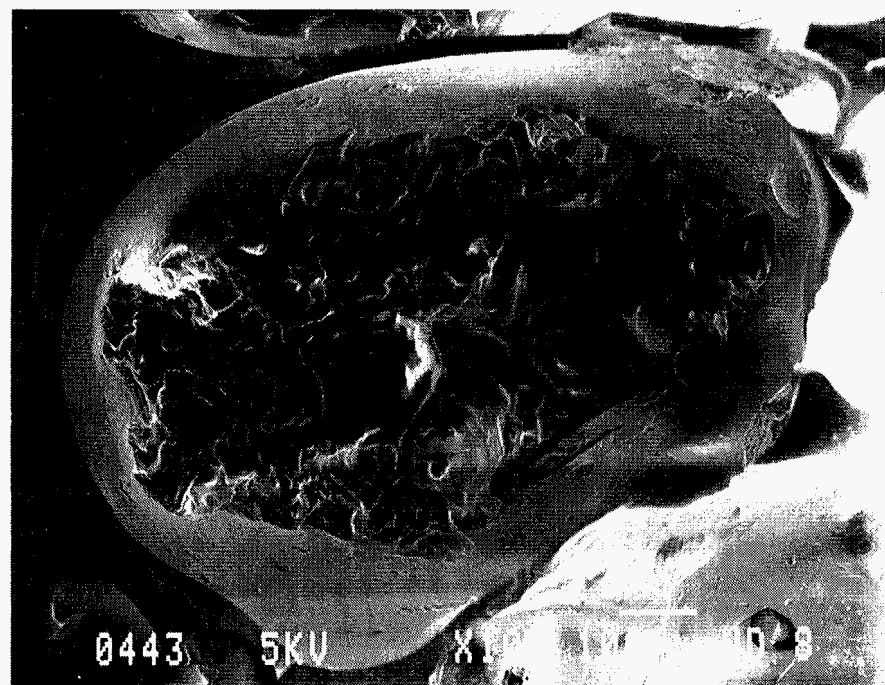
Figure 2.1-1: SEM of PTMSP-encapsulated NH₄SCN Prepared via LCED - acetone collection (8-761)

(capsule exterior)



0443 2.0KV

(cross-section)



0443 5KV X1000 0.2μ

Figure 2.1-2: SEM of PTMSP-encapsulated NH₄SCN Prepared via LCED - silicone oil collection
(8-858)

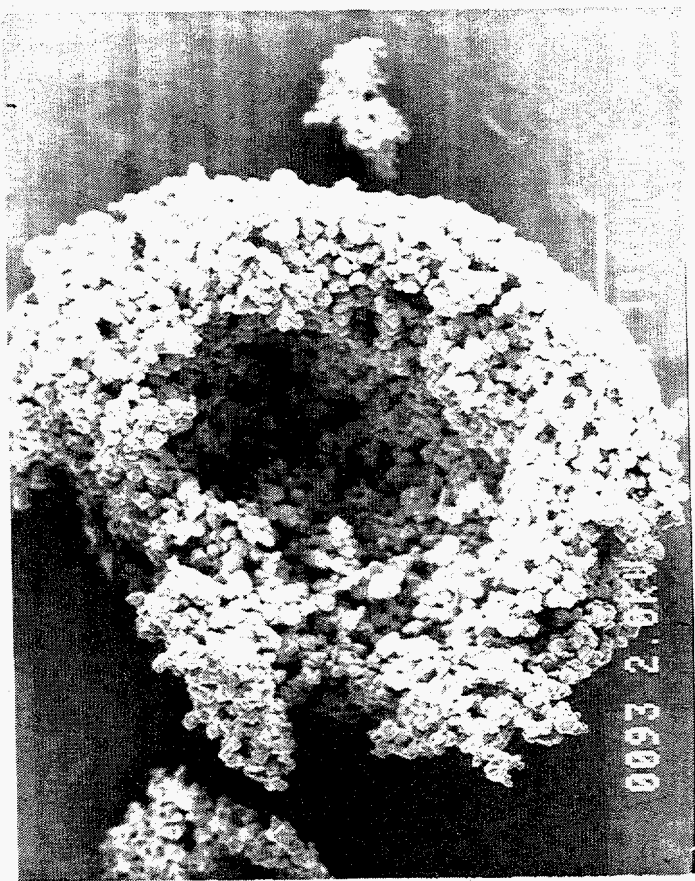
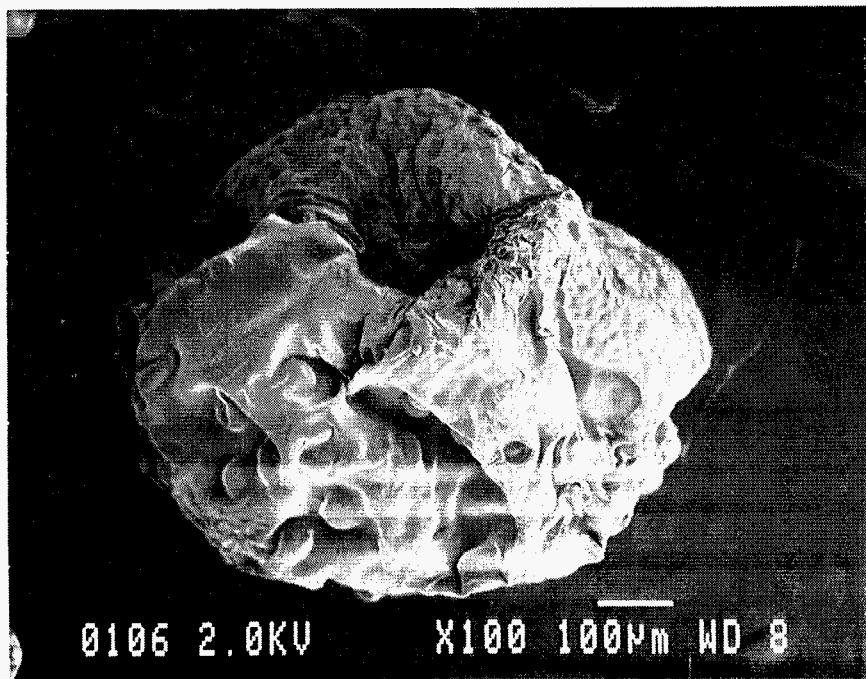


Figure 2.1-3: SEM of PTMSP-encapsulated PVAmSCN Prepared via Rotating Disk - Starch collection



(high magnification - shell)

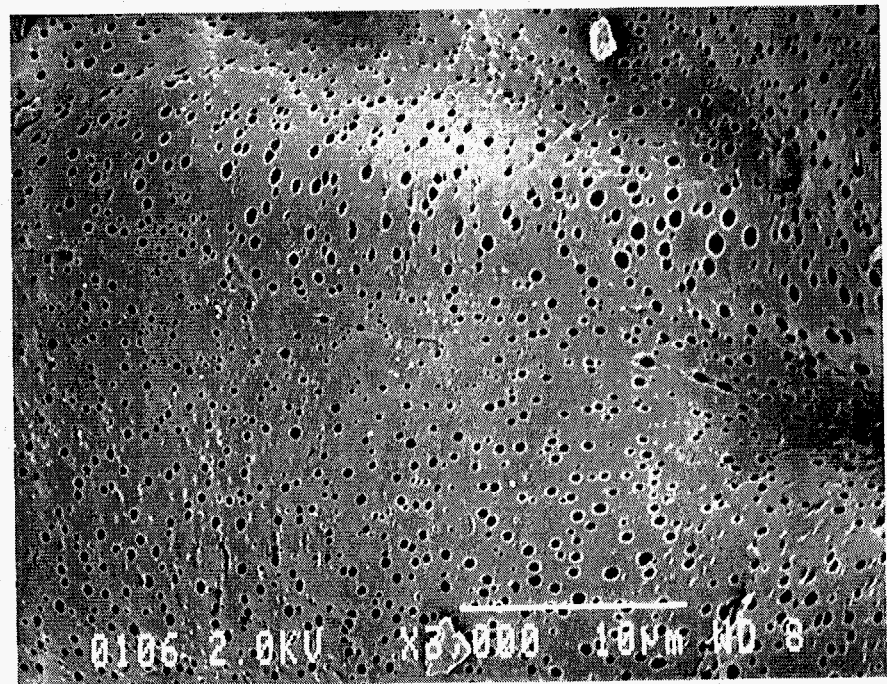


Figure 2.1-4: SEM of PTMSP-encapsulated NH₄SCN Prepared via Rotating Disk - acetone collection
(8-711)

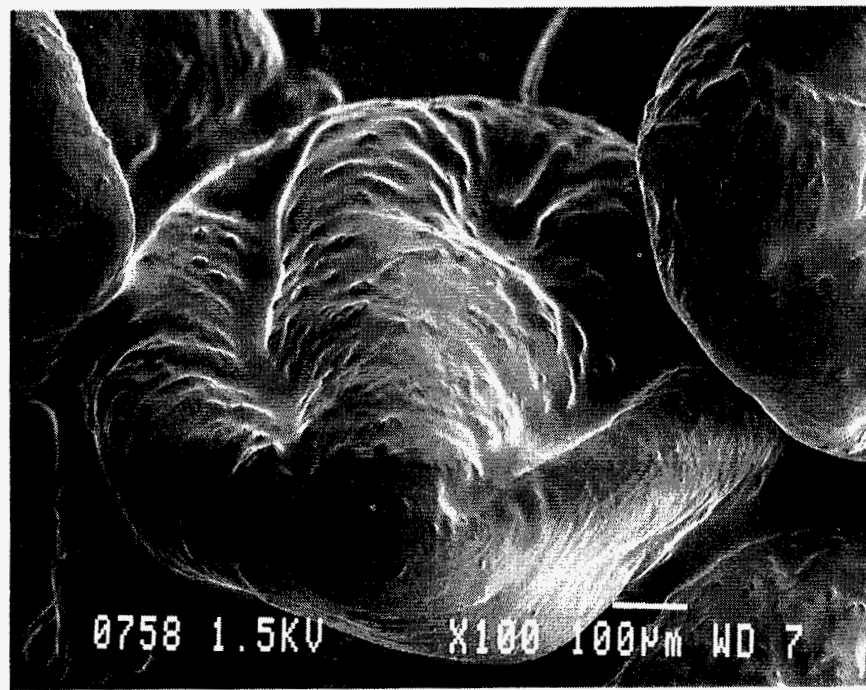


Figure 2.1-5: SEM of PTMSP-encapsulated TEAA·4H₂O Prepared via Rotating Disk - silicone oil collection
(8-970)

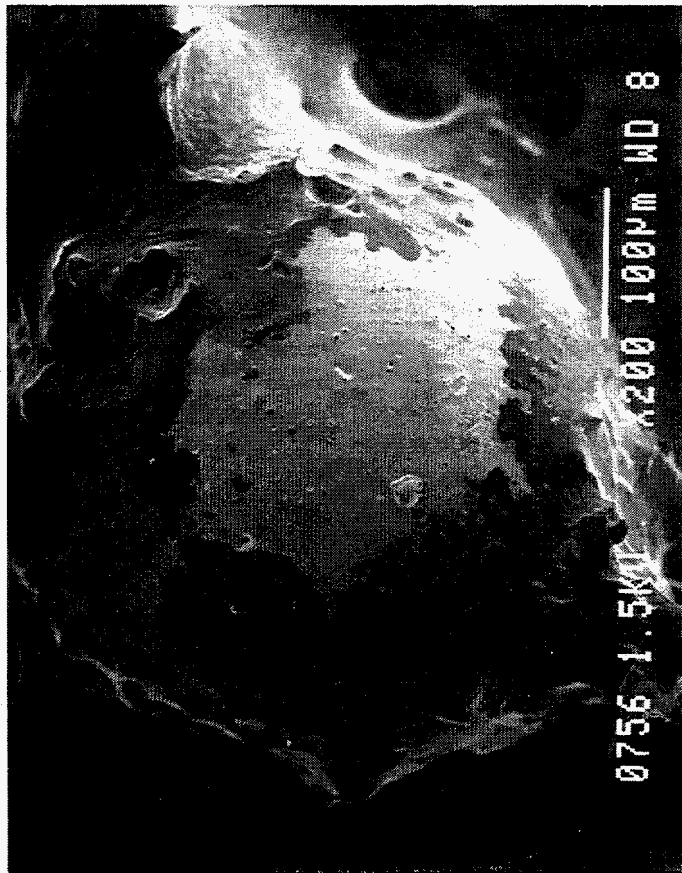


Figure 2.1-6: SEM of PTMSP-encapsulated TEAA·4H₂O Prepared via Solvent Extraction Techniques
(8-967)

Figure 2.1-7: SEM of PTMSP-encapsulated NH₄SCN Prepared via Phase Separation Techniques



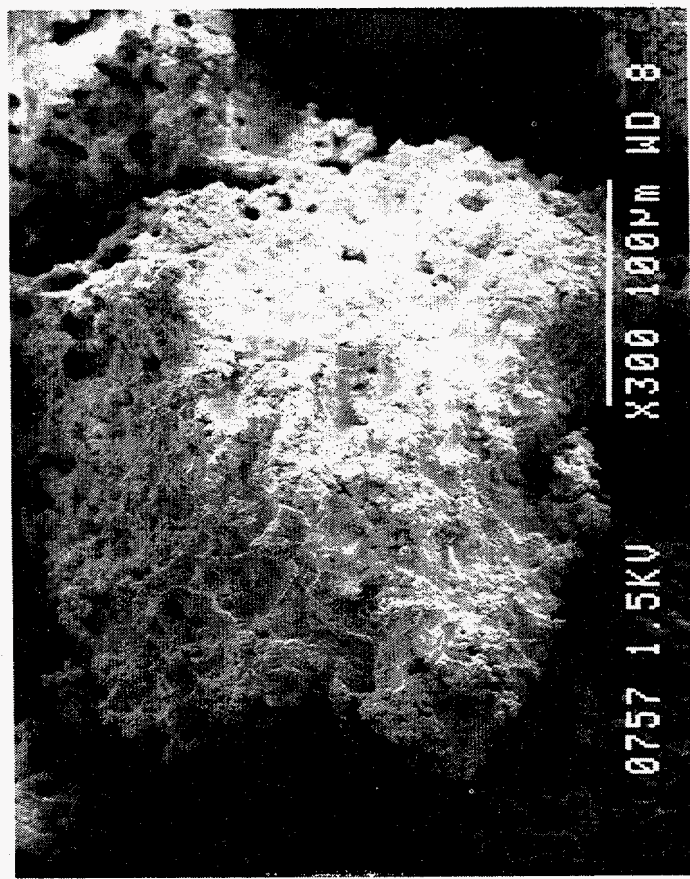


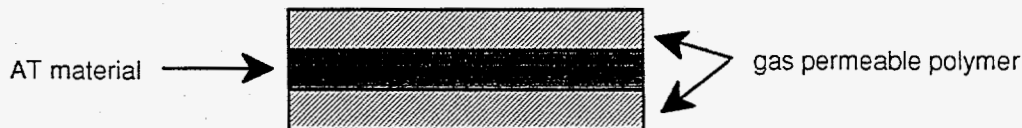
Figure 2.1-8: SEM of PTMSP-encapsulated TEAA·4H₂O Prepared via Phase Separation Techniques

3.0 Fabrication and Evaluation of CO₂-Selective MLC Membranes

Air Products and Chemicals, Inc., under an internally funded program, has developed new CO₂-selective AT materials which are amenable to multilayer composite (MLC) fabrication. Two such compositions are poly (diallyldimethylammonium fluoride), DADMAF, and poly (vinyl benzyltrimethylammonium fluoride) PVBTAF. This section covers their fabrication into multilayer composite membranes and their utility for permeating CO₂ from mixtures with CH₄ and especially H₂.

3.1 MLC Membrane Fabrication

The multilayer composite concept combines the permselective properties of an AT material with the mechanical properties of a dense film of a highly permeable but relatively nonselective support polymer as shown below.



A key issue in the MLC approach is to minimize mass transfer resistance in the support polymer layer relative to the AT material layer. In this work, we have limited the support polymers to poly(trimethylsilylpropyne), PTMSP, and poly(dimethylsiloxane), PDMS. Both are nonporous in the ordinary sense of the word. The first is a glassy polymer possessing very high gas permeability (e.g. $P_0(\text{CO}_2)=33,100$ Barrer)⁵. The latter is a rubbery polymer also exhibiting high gas permeability ($P_0(\text{CO}_2) = 3200$ Barrers)⁶.

MLC membranes were fabricated by successive casting and drying of the respective polymer solutions using blade coating techniques. PTMSP was used as a 2 wt% solution in hexane or toluene; PDMS as a 4-5 wt% solution in CH₂Cl₂. DADMAF was used as a 1-3 wt% solution in water. In some cases a proprietary surfactant was added to the aqueous phase to improve wetting properties; it is referred to as SUR-1. The films were cast onto a level, clean glass plate which had been rinsed in methanol and dried at 80°C. At all times, a shroud was kept over the membranes to limit accumulation of dust or other debris on the membrane surface. The shroud

was constantly purged with N₂. In some cases, MLCs were made which contained a microporous poly(acrylonitrile), PAN, layer supported on nonwoven polyester. The microporous PAN was produced by known fabrication techniques using a flat-sheet casting device⁷.

Some membranes were characterized using SEM. The membrane was sectioned by freezing it in liquid nitrogen. The cross-section was examined to estimate thicknesses of the layers, presence of defects, and overall appearance of the membrane. The thicknesses listed in the following tables were derived from SEM work unless otherwise noted. Representative photomicrographs of the different types of MLCs are shown in Figure 3.1-1 through 3.1-4. The layers are continuous and contain relatively few apparent flaws or defects. In some cases (see Figure 3.1-1) we observed a crack in the DADMAF layer; it is believed that this crack was introduced while preparing the specimen for microscopy.

3.2 Evaluation of CO₂-Selective MLC Membranes

The membranes were evaluated in a flowing, mixed gas permeation system described previously⁸. Additionally, both the feed and helium sweep gases could be routed through a series of bubblers, filled with water, which were placed in a thermostated bath in order to hydrate these gas streams to a chosen humidity. Alternately, the test system could be operated without a helium sweep gas. In the latter case, the permeate was collected at between 1-25 psig. It was then diluted with helium for analysis at a point downstream of the membrane (see section 4.2.2). Two feed gas mixtures was used to evaluate the membranes:

Feed Mix 1: 25.6 mol% CO₂, 74.4 mol% CH₄

Feed Mix 2: 23.0 mol% CO₂, 23.1 mol% CH₄, 53.9 mol% H₂

Unless otherwise specified, the membranes were evaluated at room temperature, in a helium-swept permeate mode with both the feed and sweep gases hydrated to the indicated dew points.

3.2.1 Stand-alone DADMAF

These DADMAF membranes did not contain any polymeric coating(s). They ranged from 30-90 μ m in thickness (as measured using a micrometer). The membranes were evaluated with feed mix #2. (except for 11273-13 which was evaluated using feed mix #1.) The permeate was swept with helium and was maintained at ~1 atm. Results are shown in Table 3.2-1.

Table 3.2-1
Evaluation of Free-standing DADMAF Membranes

Sample ID	Thickness (μm)	Membrane T (°C)	Bubbler T (°C)	P(feed) psig	Po/l (CO ₂)*	αCO ₂ /H ₂	αCO ₂ /CH ₄
11273-13	90	RT	2.5	2.3	0.024	---	---
				19.9	0.020	---	---
				55.3	0.013	---	---
11273-87	60	RT	2.5	47.4	0.028	---	---
11273-89	30	RT	2.5	36.4	0.042	---	---
				36.4	0.054	---	---
				66.3	0.039	---	---
11273-92	30	22	2.5	44.4	0.100	---	---
			5.0	44.4	0.075	---	---
			10.0	43.9	0.089	---	---
			15.0	44.0	0.103	---	---
			20.0	44.0	0.192	---	44
11273-96	40	RT	5	39.2	0.074	5.3	---
			10	39.2	0.041	2.1	3.2
			15	39.2	0.054	2.6	3.7
			20	39.2	0.083	4.4	6.9

*units of (cm³/cm²•s•cmHg)×10⁵

A dash (---) in the selectivity column indicates that H₂ and/or CH₄ was not observed in the permeate.

On average, however, only 1 in 6 of the free-standing DADMAF membranes fabricated were pinhole-free to the extent that further evaluation was even attempted. For example, membrane 11273-96 could be tested but the resulting permselective properties were poor. In the other examples, even when the selectivity was good (e.g., 11273-13), the membranes displayed poor mechanical properties and had short lifetimes.

3.2.2 PTMSP/DADMAF MLC Membranes

These membranes are a 3-layer composite consisting of a thin layer of DADMAF contained between layers of PTMSP, and were fabricated as described above. They were evaluated at room temperature using feed mixture #2 with a helium sweep gas at 1 atm. Permeation results are summarized in Table 3.2-2. The thickness, where indicated, was determined using SEM.

These MLC membranes fell into two categories. While the CO₂ permeances were relatively constant, the membranes were either very selective (i.e., only CO₂ was observed in the permeate as for 11273-18 or 11273-28) or exhibited relatively poor for an ATM selectivity (i.e., $\alpha(\text{CO}_2/\text{H}_2) < 15$). This is surprising in light of the fact that they were all cast from the same formulation by identical techniques. To investigate whether some of the membranes may have small pinholes or fabrication defects, one membrane (11638-44) was first evaluated using dry feed and sweep gases. The fact that no gases were observed to permeate under this low-humidity condition confirms the absence of gross defects. However, when this membrane was later tested under the conditions shown in Table 3.2-2, relatively poor selectivity was obtained. In some cases a postmortem of the sample indicated regions where there was poor adhesion between the PTMSP and DADMAF layers. This led us to investigate the use of surfactants.

Table 3.2-2
Evaluation of PTMSP/DADMAF/PTMSP MLC Membranes

Sample ID	Thickness (μm)	Bubbler T (°C)	P(feed) psig	Po/I (CO ₂)*	αCO ₂ /H ₂	αCO ₂ /CH ₄
11273-18	25	2.5	3.5	0.138	---	---
		2.5	35.9	0.064	---	---
		2.5	22.1	0.147	---	---
		2.5	43.5	0.102	---	---
		10.0	43.5	0.165	---	---
11273-28	25	5.0	8.0	0.284	---	---
		5.0	13.2	0.262	---	---
		5.0	30.8	0.208	---	---
		5.0	51.9	0.156	---	---
		5.0	82.1	0.131	---	---
		5.0	109.5	0.110	---	---
11273-75	42	2	12.2	0.199	---	---
		2	25.0	0.172	---	---
		2	48.3	0.125	---	---
		10	12.1	0.485	---	---
		10	25.2	0.431	26	38
		10	47.6	0.297	---	42
		20	12.1	1.94	7.4	16
11273-101	nm	2.5	40	0.225	11.3	71
		2.5	51.1	0.180	10.6	---
		2.5	62.7	0.189	8.3	65
11273-103	nm	5.0	42.7	0.240	7.9	45
11673-2	nm	5.0	40.1	0.398	5.4	33
			40.1	0.267	4.6	30
11638-44	nm	5.0	34.3	0.377	10	50
11638-46	nm	5.0	40.6	0.318	10	59

nm = not measured

*units of (cm³/cm²•s•cmHg)×10⁵

3.2.3 PTMSP/DADMAF MLC with SUR-1

A series of membranes was fabricated with SUR-1 added to the aqueous DADMAF or PVBTAF casting solution. They were then evaluated at room temperature using feed gas mix #2 and a helium sweep gas, both humidified to the dew points shown in Table 3.2-3.

Table 3.2-3
Evaluation of PTMSP/PVBTAF/PTMSP MLC with SUR-1

Sample ID	Material	Bubbler T (°C)	P(feed) psig	Po/l (CO ₂)*	αCO ₂ /H ₂	αCO ₂ /CH ₄
11638-6	PVBTAF	2.5	43.5	0.274	6.4	37
11638-7	PVBTAF	2.5	44.1	0.216	13	55
11638-8A	DADMAF	2.5	43.6	0.320	7.6	26
11638-8B	DADMAF	2.5	47.8	0.290	6.7	28

*units of (cm³/cm²·s·cmHg) × 10⁵

Still, the selectivity was less than expected. A postmortem indicated better adhesion but did not rule out the possibility of small regions where adhesion might still be poor. This seems increasingly likely in light of the above data which demonstrates that the addition of this surfactant (at this level) does not appear to improve the permselectivity.

3.2.4 MEM213/DADMAF MLC Membranes with SUR-1

MEM213 is a silicone rubber/polycarbonate copolymer available from General Electric Corp. in flat sheets of 1 and 2 mil thickness. MLC membranes were fabricated using MEM213 as the support or "encapsulating" polymer. Results from the evaluation of these membranes are reported in Table 3.2-4. These membranes do not exhibit attractive separation properties.

Table 3.2-4
Evaluation of MEM213/DADMAF/MEM213 MLC Membranes

Sample ID	Material	Bubbler T (°C)	P(feed) psig	P _{o/l} (CO ₂) [*]	αCO ₂ /H ₂	αCO ₂ /CH ₄
11638-11	DADMAF	2.5	46	0.332	4.7	8
11638-14	DADMAF	2.5	44.6	0.239	6.1	28
11638-16	DADMAF	2.5	44.0	0.350	6.5	12

*units of (cm³/cm²•s•cmHg) x10⁵

3.2.5 PDMS/DADMAF/PDMS MLC Membranes

These membranes consist of a layer of DADMAF contained between layers of poly(dimethylsiloxane). It was essential to use SUR-1 in order to obtain adequate wetting between the polymer and DADMAF solution. The surfactant level was held constant in all subsequent membranes except where noted. All membranes were basically identical in preparation. Permeation test results are shown in Table 3.2-5. The first membrane tested, 11638-38, had relatively poor selectivities; examination of the membrane after permeation testing revealed wrinkles or creases in the membrane which may have resulted from delamination of the layers. Membrane 11638-47-1 was initially tested using dry feed (feed mix #2) and sweep gases; relatively small amounts of CO₂ and CH₄ were observed in the permeate. When the gas streams were later humidified to 5°C, the membrane did not seal completely and exhibited poor selectivity (Table 3.2-5). Membrane 11638-47-2 (a second membrane cut from a larger section of 11638-47) exhibited no detectable H₂ or CH₄ permeation at the test condition. During the first 2 days of operation, membrane 11638-50 exhibited a decreasing CO₂ flux; a small amount of CH₄, but no H₂, was observed in the permeate. Eventually, a steady state was reached at which point the CO₂ flux remained constant but neither H₂ or CH₄ was observed in the permeate. This steady-state data is reported in Table 3.2-5.

Table 3.2-5
Evaluation of PDMS/DADMAF/PDMS MLC Membranes

Sample ID	Bubbler T (°C)	P(feed) psig	Po/l (CO ₂)*	αCO ₂ /H ₂	αCO ₂ /CH ₄
11638-38	5	52.4	0.19	6.6	58
	10	52.4	0.32	7.2	34
11638-47-1	5	35.0	0.179	7.3	34
11638-47-2	5	34.4	0.196	---	---
11638-50	5	51.1	0.183	---	---

*(cm³/cm²•s•cmHg)×10⁵

After the above data was collected, the test of 11638-50 was continued for an additional 23 days. No indication of instability or flux decline was observed. During this extended test feed mix #1 was used and the feed and helium sweep gases were humidified to 5°C; the membrane was maintained at room temperature. The total pressure in the feed stream (and hence the CO₂ partial pressure) was varied during this test. No CH₄ was detected in the permeate at any of the pressures studied. The steady-state data for each experimental condition is shown plotted in Figure 3.2-1. The CO₂ permeance exhibits a characteristic of many facilitated transport membranes; that is, the CO₂ permeance decreases with increasing CO₂ partial pressure in the feed stream.

Based on the promising results of sample 11638-50, PDMS/DADMAF/PDMS MLC membranes were investigated further. Specifically, the effects of temperature and dew point were examined. In this experiment the feed gas (mixture #1) was maintained at 38.6 psig. Results (membrane 11638-54-2, thickness 30-35μm) are reported in Table 3.2-6.

At a constant temperature of 22°C, the CO₂ permeance varies linearly with dew point in the range of 2-20°C. For a constant dew point of 20°C, CO₂ permeance decreases with increasing membrane temperature. We speculate that this is a result of an equilibrium between water vapor in the feed gas stream and water absorbed in the DADMAF layer. At higher dew points, more water is absorbed by DADMAF and diffusion in this layer becomes more facile. At higher temperatures, the equilibrium is shifted in the direction of water vapor. The DADMAF layer, now depleted of water, becomes a better barrier and permeance decreases.

Figure 3.2-1

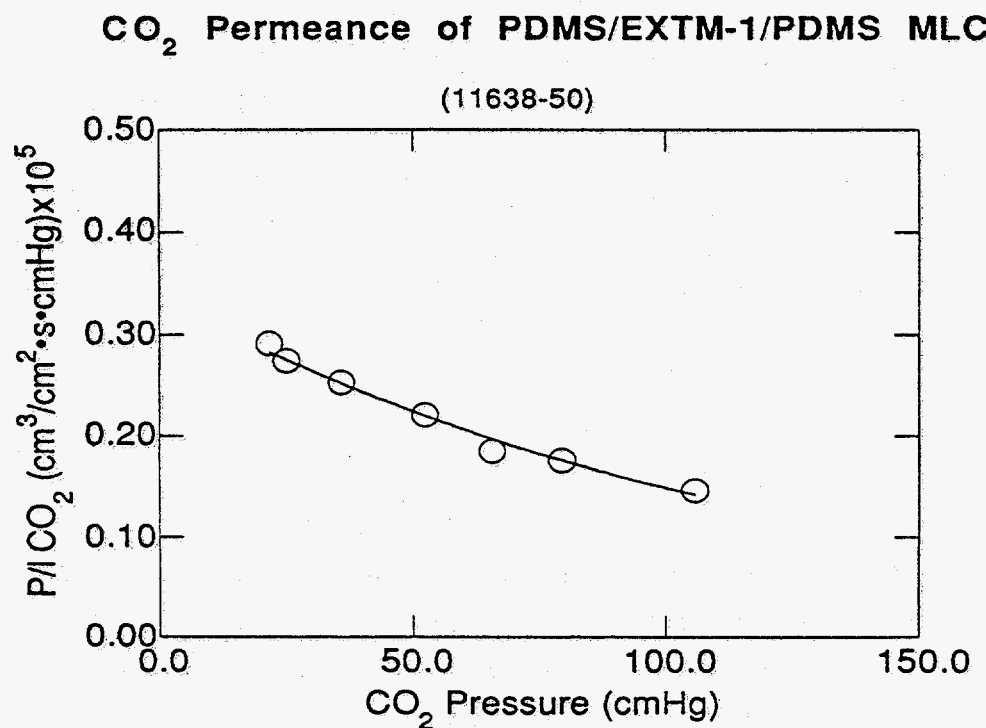


Table 3.2-6
Effect of Dew Point and Temperature on PDMS/DADMAF/PDMS MLC Membrane

Membrane T(°C)	Dew Point (°C)	P ₀ /I (CO ₂)*
22	2.0	0.138
22	4.0	0.184
22	10.4	0.311
22	14.7	0.377
22	20.1	0.535
40	20.1	0.421
50	20.1	0.175
60	20.1	0.108
70	20.1	0.068

*($\text{cm}^3/\text{cm}^2 \cdot \text{s} \cdot \text{cmHg} \times 10^5$)

To further investigate the role of H₂O vapor in the permeation process, the PDMS/DADMAF/PDMS MLC was evaluated at room temperature with various combinations of wet and dry feed and helium sweep gas streams. In these experiments, the "wet" condition is 5°C. The feed gas was mix #1 at 39.3 psig. The data was collected in the order listed in Table 3.2-7. The last line of the data shows that the dew point was raised to 20°C. In no cases was CH₄ observed in the permeate stream.

Table 3.2-7
Effect of Gas Stream Hydration of Membrane Performance

Feed Gas	Sweep Gas	P _{0/I} (CO ₂) [*]
wet	wet	0.241
wet	dry	0.022
wet	wet	0.235
dry	wet	0.140
wet	wet	0.222
wet (20°C)	wet (20°C)	0.609

^{*}(cm³/cm²•s•cmHg)×10⁵

Only the use of a dry sweep gas appears to significantly decrease the CO₂ permeance; the loss of CO₂ permeance can be restored by raising the dew point back to its original value. As expected, CO₂ permeance is much larger at the higher (20°C) dew point.

Of the membranes studied, the PDMS/DADMAF/PDMS MLC membranes have exhibited the best CO₂ permselective properties. A CO₂ permeance of ca 0.2 Barrers/cm (x10⁵) translates into a standard permeability of 70 Barrers (assuming an AT layer 35μm thick). In a "good" membrane no H₂ or CH₄ was detected under the test conditions and thus no selectivity can be calculated. We have recently upgraded the analytical capabilities of this test system to increase the sensitivity towards H₂ by ≈10x. The PDMS/DADMAF/PDMS MLC membranes listed below were evaluated using this new equipment. The feed stream was mix #2 and the membranes were tested at room temperature. Results are shown in Table 3.2-8.

Now, for the first time, we have been able to unambiguously determine $\alpha(\text{CO}_2/\text{H}_2)$ and

$\alpha(\text{CO}_2/\text{CH}_4)$ of these membranes. However, reproducibility was not good. Even for membranes tested under the same conditions (compare 11638-82-1 with 11638-88), the selectivity varied by a factor of 2. We also note that a higher CO_2 permeance was accompanied by a lower selectivity for membranes of approximately equal thickness (11638-88 and 11638-92-1).

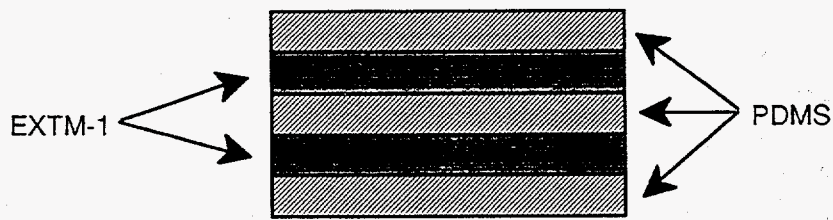
Table 3.2-8
Evaluation of MLC Membranes with Improved Analytical System

Sample ID	Bubbler T (°C)	P(feed) psig	P _{o/l} (CO ₂)*	$\alpha\text{CO}_2/\text{H}_2$	$\alpha\text{CO}_2/\text{CH}_4$
11638-82-1	5	46.6	0.259	25	73
11638-85-1	10	37.7	0.336	29	90
	20	37.7	0.447	14	32
11638-87-1	10	44.7	0.445	15	64
11638-88	10	44.3	0.294	25	79
	5	44.3	0.196	44	130
11638-92-1	5	45.0	0.213	10	40

*(cm³/cm²•s•cmHg)×10⁵

The variability in flux and selectivity is still somewhat puzzling. It is not readily apparent why some membranes possess very good selectivity and why some are relatively poor. We note that the lower selectivities are not the result of a hole in the usual sense because the selectivities are much greater than 1. To investigate the possible role of very small flaws or defects in the membranes we performed several experiments. In one group we examined the effect of multiple DADMAF layers. This was done in two ways. In the first, two 3-layer MLC membranes were fitted into the test cell at the same time (11638-95-1). If there were small defects, the probability of one in each membrane lining up is very low. If the membranes were defect-free, one would expect a lower CO_2 permeance (in proportion to the thickness of the DADMAF layer) but no change in selectivity. Results are shown in Table 3.2-9. The CO_2 permeance fell by a factor of 2. (Compare with 11638-95-1 which contains only 1 piece of the same 3-layer composite.) This is expected since the DADMAF layer was approximately twice as thick. More importantly sample 11638-95-1 exhibited improved $\alpha(\text{CO}_2/\text{H}_2)$ and $\alpha(\text{CO}_2/\text{CH}_4)$. This result strongly

suggests that the membranes contain microscopic flaws which detract from the intrinsic selectivity of DADMAF. In a similar experiment, a 5-layer MLC membrane was fabricated (11638-102-1). Its structure is shown below (SEM in Figure 3.1-4).



The CO₂ permeance was approximately half that of its 3-layer counterpart but the selectivity was much improved. These results support the theory that adhesion between the layers is less than adequate or that microscopic cracks, dust or other particulate matter give rise to flaws and defects.

In the last set of experiments, the amount of SUR-1 was increased by a factor of 4. The results on 3-layer composite MLCs are presented in Table 3.2-9 (12110-2-1 and 12110-3-1). The CO₂/H₂ selectivity of 50-80 is the highest reported. (Polymer membranes typically have CO₂/H₂ selectivity <1). The results strongly suggest the need to keep good adhesion between the various layers. Future work will address the surfactant level and its effect on membrane performance as well as screen different surfactants.

3.2-6 Evaluation of PDMS/DADMAF MLC Membranes at Elevated Permeate Pressure

There is limited permeation data on these CO₂-selective MLC membranes taken at elevated permeate pressures. However, the data that does exists suggests that the membranes will be effective at permeate pressures approaching 20 psia. Table 3.2-10 contains data for two MLC membranes: 11273-54, a PTMSP/DADMAF/PTMSP composite and 11638-66, a PDMS/DADMAF/PDMS composite. In the first case, the membrane (7 μ m DADMAF layer) was tested with feed mix #1 and gas streams humidified to 10°C. In the first two entries, a helium sweep gas was used. In the third entry, the permeate gases were collected at 19.2 psig. The data show that membrane performance is comparable in the two cases.

Table 3.2-9
Investigation of Flaws and Defects

Sample ID	Bubbler T (°C)	P(feed) psig	Po/l (CO ₂)*	αCO ₂ /H ₂	αCO ₂ /CH ₄
11638-95-1 2 pieces	5	42.9	0.0973	42	---
11638-95-1 1 piece	5	41.1	0.176	31	49
	10	41.1	0.288	22	85
	15	41.1	0.378	12	37
11638-102-1 5 layer MLC	5	42.8	0.101	65	---
	5	67.2	0.0801	55	---
	5	40.6	0.0941	62	---
	10	40.6	0.161	38	---
12110-2-1	5	10.5	0.183	81	---
	5	26.4	0.155	76	---
	5	41.4	0.145	81	---
	5	68.7	0.120	69	---
	5	108.8	0.087	53	---
12110-3-1	5	16.0	0.203	67	---

*(cm³/cm²·s·cmHg)×10⁵

Table 3.2-10
Effect of Permeate Pressure on Membrane Performance

Sample ID	P _f (CO ₂) psig	P(perm) psig	Po/l (CO ₂)*
11273-54	56	0	0.0481
	85.9	0	0.0453
	85.8	19.2	0.0440
11638-66	40.5	0	0.202
	40.5	0.9	0.176

*(cm³/cm²·s·cmHg)×10⁵

3.3 SUMMARY/STATUS

We have demonstrated that it is possible to fabricate MLC membranes from DADMAF and PDMS. We have shown that these membranes can be highly selective for CO₂ over H₂ (CO₂/H₂)=80) if adequate adhesion is maintained between the layers. The membranes appear to function via a facilitated transport mechanism. They are able to withstand a transmembrane pressure of at least 90 psi and are stable for at least 3 weeks of continuous testing. Water vapor plays an important role in the functioning of the membranes; its effect is being studied further.

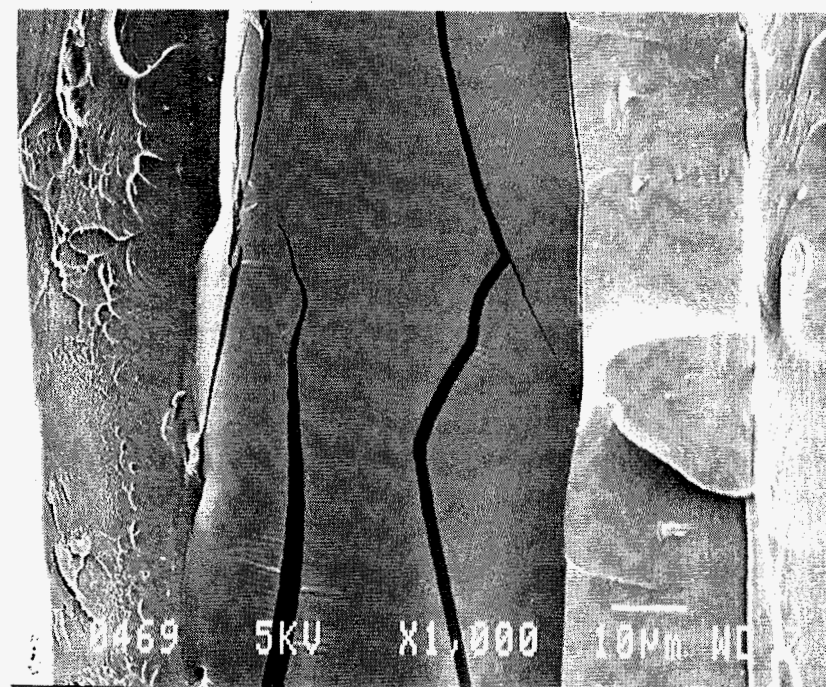


Figure 3.1-1: Scanning Electron Microscopy of PTMSP/EXTM-1/PTMSP MLC - cross-section (11273-75)

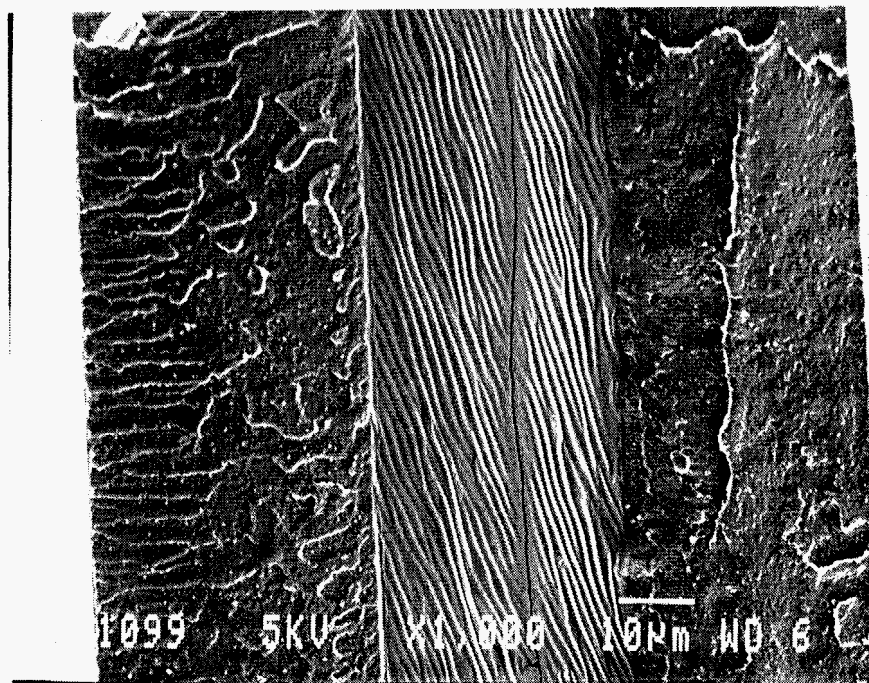


Figure 3.1-2: Scanning Electron Microscopy of PDMS/EXTM-1/PDMS MLC - cross-section (11638-50)

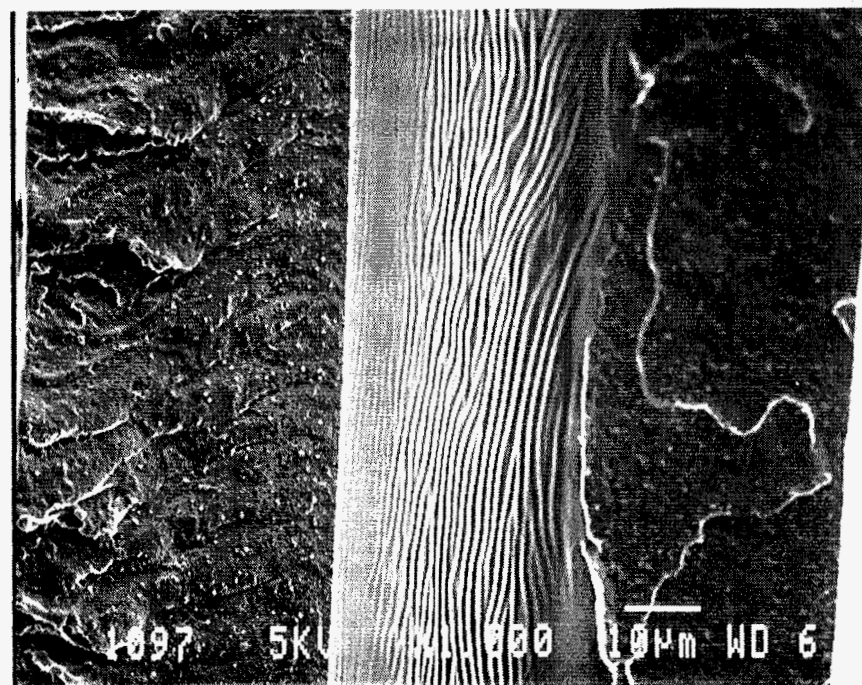


Figure 3.1-3: Scanning Electron Microscopy of PDMS/EXTM-1/PDMS MLC after Testing - cross-section (11638-50)

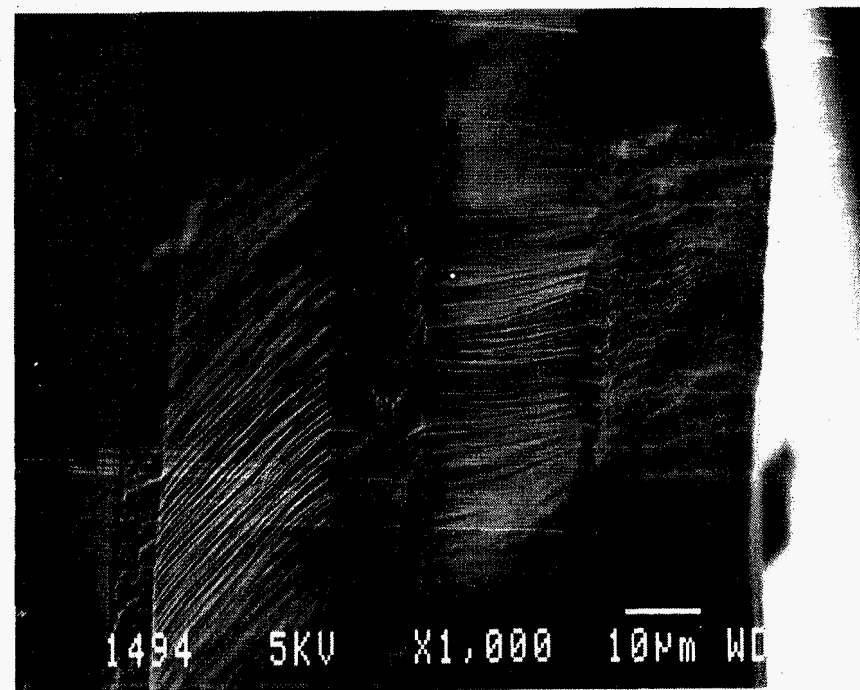


Figure 3.1-4: Scanning Electron Microscopy of PDMS/EXTM-1/PDMS/EXTM-1/PDMS 5-layer MLC - cross-section (11638-102-1)

4.0 Evaluation of NH₃-Selective MLC Membranes

4.1 Process Application/Evaluation: NH₃ Recovery in Ammonia Synthesis

A major market for NH₃-selective membrane technology is in ammonia synthesis applications. As described previously⁹ ammonia-selective membranes could be used in at least three scenarios. Two anticipated major applications are given below. Air Products has conducted a cursory examination the two process applications (cases A and B) following inquiries from two major suppliers of ammonia plants and equipment. This preliminary analysis addressed the technical feasibility of integrating membrane-based separations into ammonia synthesis plants. Membrane properties and lifetimes were projected from lab data. A more detailed analysis will be conducted using permeation data collected under task 3 of the program. In these analyses the membranes were used:

- A) As part of a debottlenecking/refrigeration hybrid retrofit to existing ammonia plants and/or in construction of new plants. In this case, the membrane would be placed immediately downstream of the converter to reduce the load on the refrigeration system. (Figure 4.1-1) This scheme would most likely be used in connection with upgrading an older reactor, i.e., increase conversion from 12.8% to 15.9% (an increase in yield of \approx 24%). In order to recover the additional product by conventional means, the refrigeration loop must be significantly expanded. Alternatively, the hybrid scheme shown in Figure 4.1-1 could be used where only a portion of the NH₃ is removed via a membrane. The reject stream from the membrane, which has a similar composition to that of the old converter, would then be sent to the existing refrigeration system which, in this hybrid scheme, requires only a minimal expansion. From an economic viewpoint, the NH₃-selective membrane should be able to compete with conventional recovery methods because of the projected savings in refrigeration system upgrade and operating costs (i.e. power consumption).
- B) As a means to effect total NH₃ recovery; that is, a cascading series of membrane stages are placed immediately downstream of the converter to remove ammonia to the same extent as in the conventional, refrigeration-based process. This eliminates the need for a large refrigeration system. This general concept was initially proposed by Brubaker and Kammermeyer in 1954¹⁰ but has not been

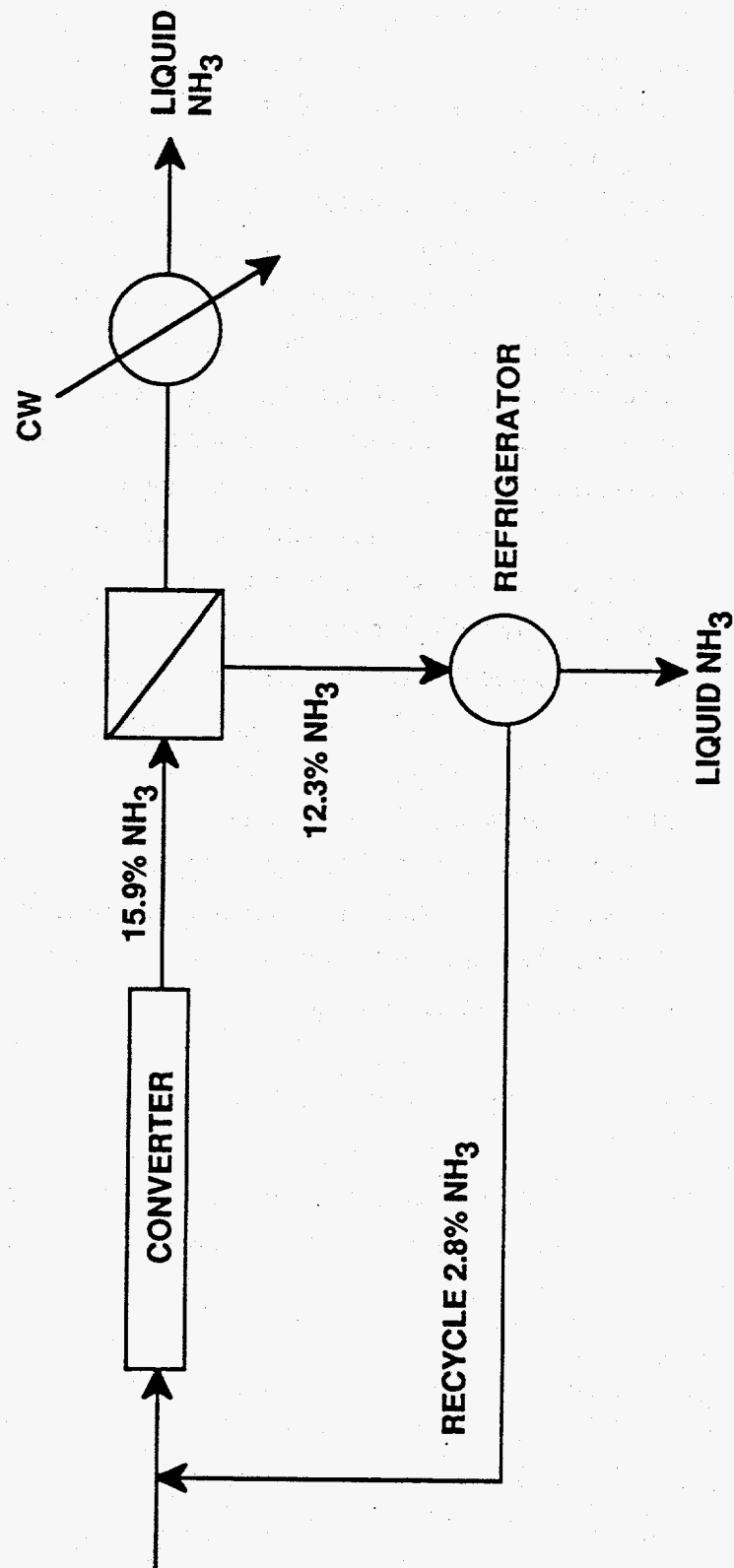


Figure 4.1-1: Debottlenecking Hybrid Scenario Applied to Ammonia Synthesis

implemented because membranes with adequate NH₃/H₂ selectivity had not been identified. This case involves replacing the current ammonia separation scheme with a membrane system to effect the same NH₃ recovery achieved in the conventional purification system. The current recovery system reduces the NH₃ concentration in the syngas stream from 15.8% to 2.8%. Product NH₃ is recovered by cooling, first with water and ultimately with liquid NH₃ cycled from the ammonia refrigeration loop. The reject stream, containing 2.8% NH₃, is recycled to the converter. In the scheme proposed by APCI (Figure 4.1-2), this same separation is effected in three membrane stages. Permeate gas from the second and third stages are compressed to 225 psia and mixed with first-stage permeate and then liquified against cooling water. This is possible only because the permeate stream is essentially pure NH₃ (due to the high selectivity of the membrane) and as such can be liquified at 225 psia and 100°F. While approximately 50% of the product is recovered at 100°F (38°C) it is interesting to note that raising the permeate pressure to 227 psia increases NH₃ recovery in the condenser to 66%, and that cooling the stream further to 95°F (35°C) increases the amount of NH₃ liquified to 83%. At this time Case B appears marginally attractive. Although the use of a membrane results in a substantial power savings over refrigeration, it is offset against the additional capital cost of the two-stage compressor as well as the large membrane area required to achieve the separation. However, because there is a large net power savings, both parties continue to show interest in this scenario.

4.1.1 Membrane Operating Parameters at Process Conditions - NH₃ Synthesis

The following sets of conditions were used in the process analysis described above. They provided the basis for evaluating lab-scale membranes under "process conditions" as described in the test plan in section 4.1.2.

Feed/Permeate Conditions: In Case A we determined the separation achievable when the permeate stream from the membrane is set to 222 psia to allow high purity NH₃ to be condensed against cooling water. In case B, the permeate pressure was set to 225 psia. The NH₃ synthesis stream from the converter (feed stream to the membrane) was set at a pressure of 1980 psia with the gas composition shown in Table 4.1-1. These conditions are typical in state-of-the-art NH₃ synthesis plants.

Table 4.1-1
NH₃ Synthesis Converter Effluent Composition

<u>Component</u>	<u>Mol %</u>	<u>Partial Pressure (psia)</u>
Ammonia	15.85	313.8
Hydrogen	54.83	1,085.5
Nitrogen	20.24	400.8
Methane	6.66	132.0
<u>Argon</u>	<u>2.42</u>	<u>47.9</u>
Total	100	1,980

Operating Temperature: In this analysis, 150°F (66°C) was chosen as the operating temperature for the membrane. In order to choose an appropriate working temperature, the dew points of both the feed and permeate streams had to be determined. The NH₃ dew point in the feed stream is about 99°F (40°C). The relationship of dew point to ammonia partial pressure for high purity ammonia streams (90-99 mol% NH₃) is shown in Figure 4.1-3. According to the curve, at a permeate pressure of 222 psia, NH₃ will condense between 100 and 104°F (38 and 40°C) which is considered the lower limit for cooling water. The operating temperature of the membrane must be set greater than 100°F (37°C) to avoid condensation of NH₃ in both the feed and permeate streams. In addition, gas permeating the membrane will cause some Joule-Thompson cooling, which is estimated to be 5°F (3°C) for this case and 15°F (8°C) for Case B. Accordingly, 150°F (66°C) was chosen as the operating temperature.

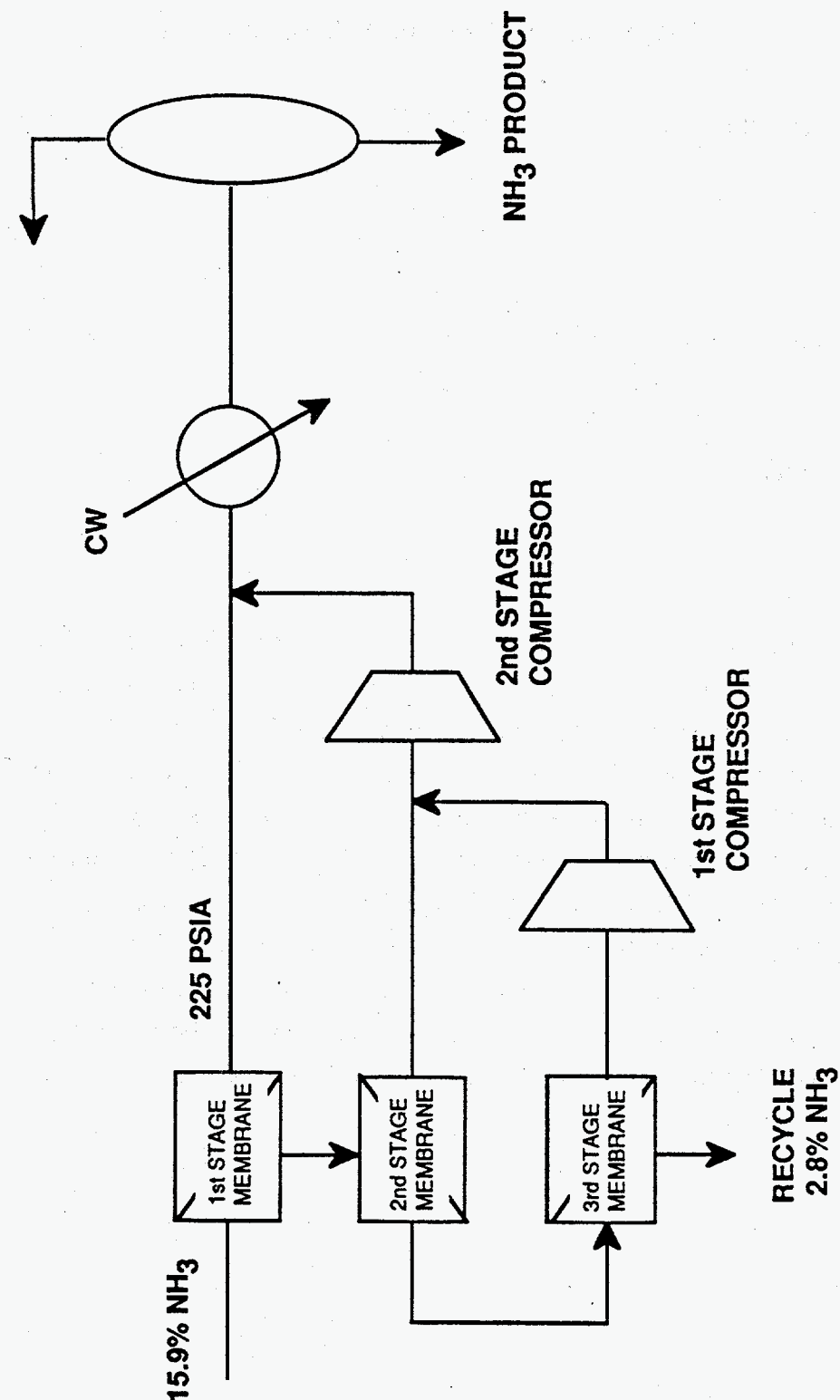


Figure 4.1-2: Total Ammonia Recovery from Ammonia Synthesis via Membranes

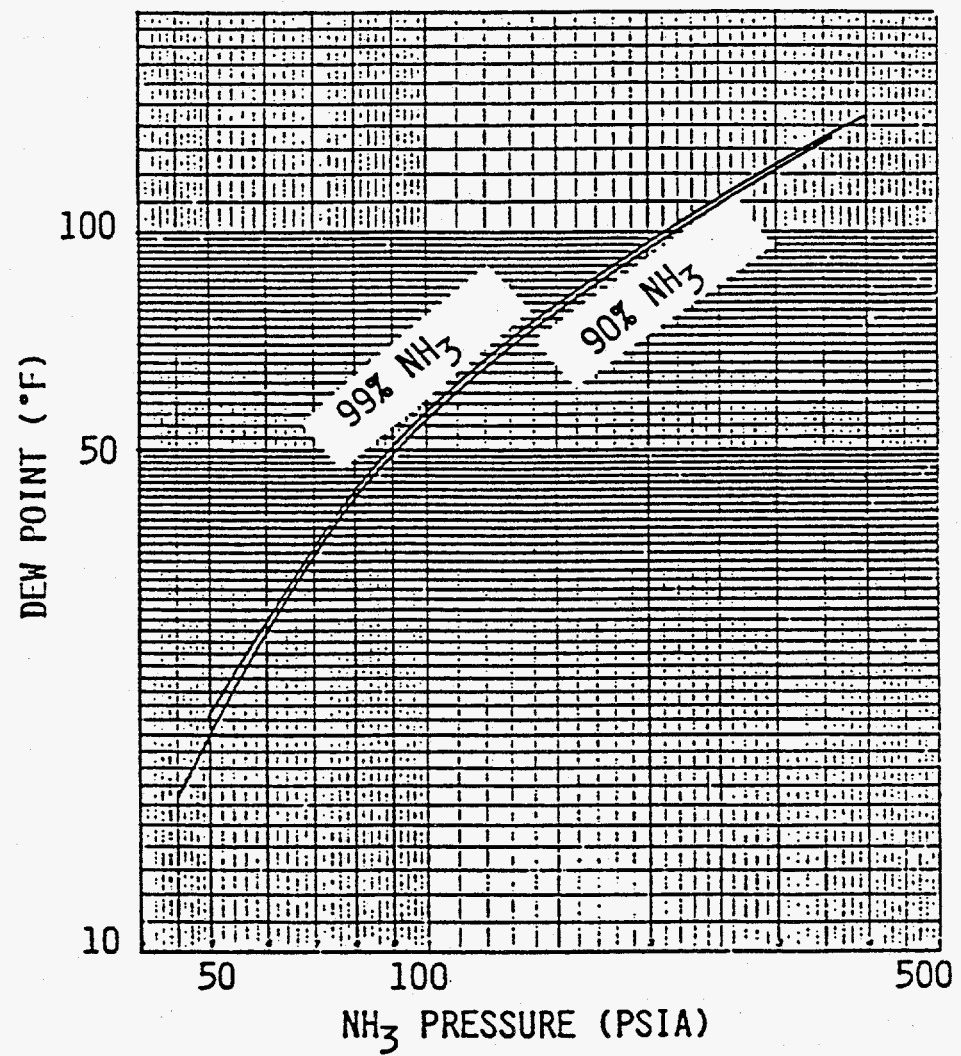


Figure 4.1-3: Relationship of Dew Point to Pressure for High Purity Ammonia Streams

4.1.2 Membrane Test Plan

Based on the above information a test plan was developed for evaluating lab-scale, NH₃-selective membranes under simulated process conditions. For these tests, N₂ was substituted in the feed gas stream for the small amounts of methane and argon found in the actual process. This considerably reduced the complexity of the permeate gas analysis system.

Laboratory-scale membranes were to be evaluated for NH₃, N₂ and H₂ permeability under conditions shown in Table 4.1-2. Successful membrane operation at these conditions represent milestones for the program. Data collected near these conditions can be used in APCI-developed computer models to evaluate the feasibility of the processes proposed in Cases A and B. Experiments were to be conducted in the order shown in Table 4.1-2; that is, in order of increasing experimental complexity and severity of operating conditions. In addition, membranes were to be tested at intermediate pressures to verify membrane integrity before "process conditions" were reached. These experiments would typically consist of 3-6 measurements of permselectivity at the same temperature as the milestone test, but would begin at lower total stream pressures. After performance is verified at one set of conditions, the total feed stream pressure would be increased. By repeating this process we would ultimately arrive at the milestone test. Sufficient data was collected at each set of conditions to establish steady-state operation (usually 24-48 hrs).

4.2 Membrane Permeation Test System

Membrane permeation test equipment was upgraded to produce conditions (feed and permeate gas, temperature, etc.) typical of the end-use application for APCI NH₃- and CO₂-selective Active Transport membranes; namely, NH₃ recovery from the synthesis loop of an ammonia synthesis plant and CO₂ removal from reformer effluent in methane steam reformers. The test equipment, which is currently configured for NH₃ permeation tests, can be used for either application, after minor changes which are discussed below.

4.2.1 Flow Diagram

A process flow diagram (PFD) for the permeation system is shown in Figure 4.2-1. The unit consists of a) a feed gas blending section, b) an oven containing the membrane and cell and c) an analytical system. The feed gas stream is generated by sparging a metered flow of a preblended mixture of N₂ in H₂ from a high pressure "BX" cylinder (CYL-1) through a second cylinder

(CYL-2) which contains liquid NH₃. (This cylinder, CYL-2, is removed from the system for filling with NH₃.) An expanded view of the sample cylinder (CYL-2) inlet/outlet connections is shown in Figure 4.2-2. The concentration, or partial pressure, of NH₃ in the feed gas is regulated by the temperature of CYL-2 via HTR-1. The ternary blend is then routed through a preheater to the membrane cell which is housed in the oven. The pressure of the feed stream is maintained at a pressure set via BPR-2 and measured by PT-4. The NH₃ is water-stripped from the reject stream before it is discharged to the atmosphere. The permeating gases are collected at a pressure set at BPR-3 and measured by PT-5. As the permeant gas bleeds across BPR-3 it is picked up in a metered flow of helium and routed to a gas chromatograph for analysis. The analytical system (gas chromatograph, integrator etc.) is as reported previously¹¹.

The oven was custom built by APCI support services. It is constructed of aluminum with 2" of insulation in the walls. It was specifically designed to minimize temperature gradients within the oven space and to maintain constant temperature at 30-100°C. For safety, the oven is constantly purged with N₂ to prevent the build-up of combustible gases inside the oven in the event that a leak should occur in the test equipment. Additionally, the N₂ flow is part of a safety feedback system; if the N₂ flow fails or is impeded, the system will automatically revert to shutdown mode. This is just one of the many safety features incorporated into the design to render it safe for unattended operation. The oven, test equipment analytical system, and associated equipment are shown in Figure 4.2-3. For safety reasons the unit is housed inside a "Process Development High Pressure Cell"

4.2.2 Electrical Diagram

"Ladder" diagrams detailing electrical connections are shown in Figure 4.2-4. The majority of these components are mounted in a cabinet (Figure 4.2-5) located outside the Process Development Cell.

MEMBRANE TEST PLAN

<u>Feed Stream</u>	<u>Membrane Temperature</u>	<u>Feed Stream Composition*</u>				<u>Permeate Stream</u>	
		<u>PNH₃</u>	<u>PN₂</u>	<u>PH₂</u>	<u>P_{tot}</u>	<u>P_{total}</u>	<u>PNH₃</u>
3rd stage reject	139°F	55	666	1244	1965	40	39
3rd stage feed	139°F	127	642	1200	1970	40	39
2nd stage feed	146°F	239	605	1131	1975	100	98
1st stage feed	150°F	314	580	1086	1980	225	220

• psia

TARGET PERFORMANCE

$$P_{o/f} \text{ NH}_3 = 40$$

$$\alpha(\text{NH}_3/\text{N}_2) > 1000$$

$$\alpha(\text{NH}_3/\text{H}_2) > 1500$$

Table 4.1-2: Membrane Test Plan and Target Membrane Performance

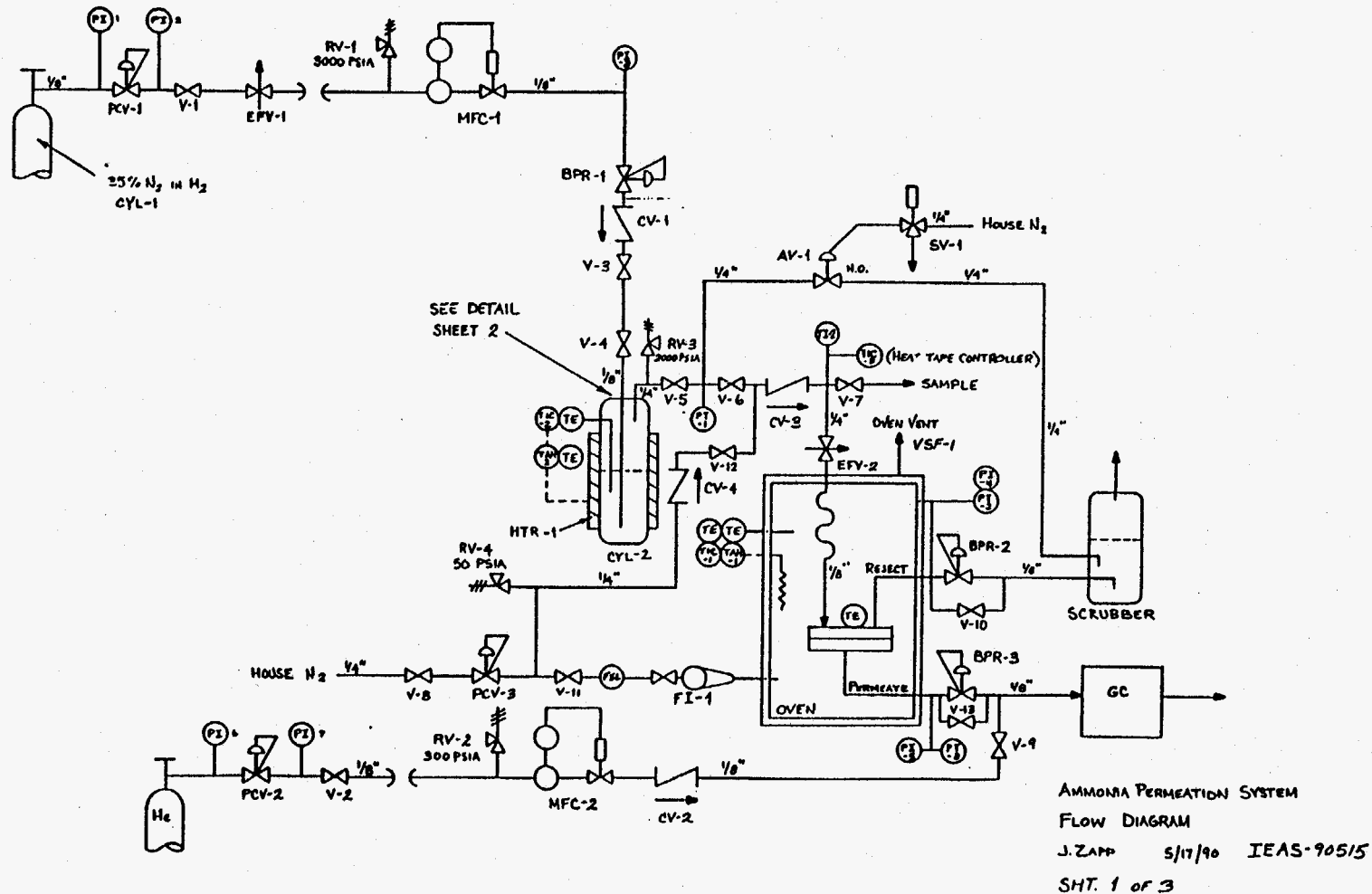


Figure 4.2-1: Process Flow Diagram - High Pressure Membrane Test System

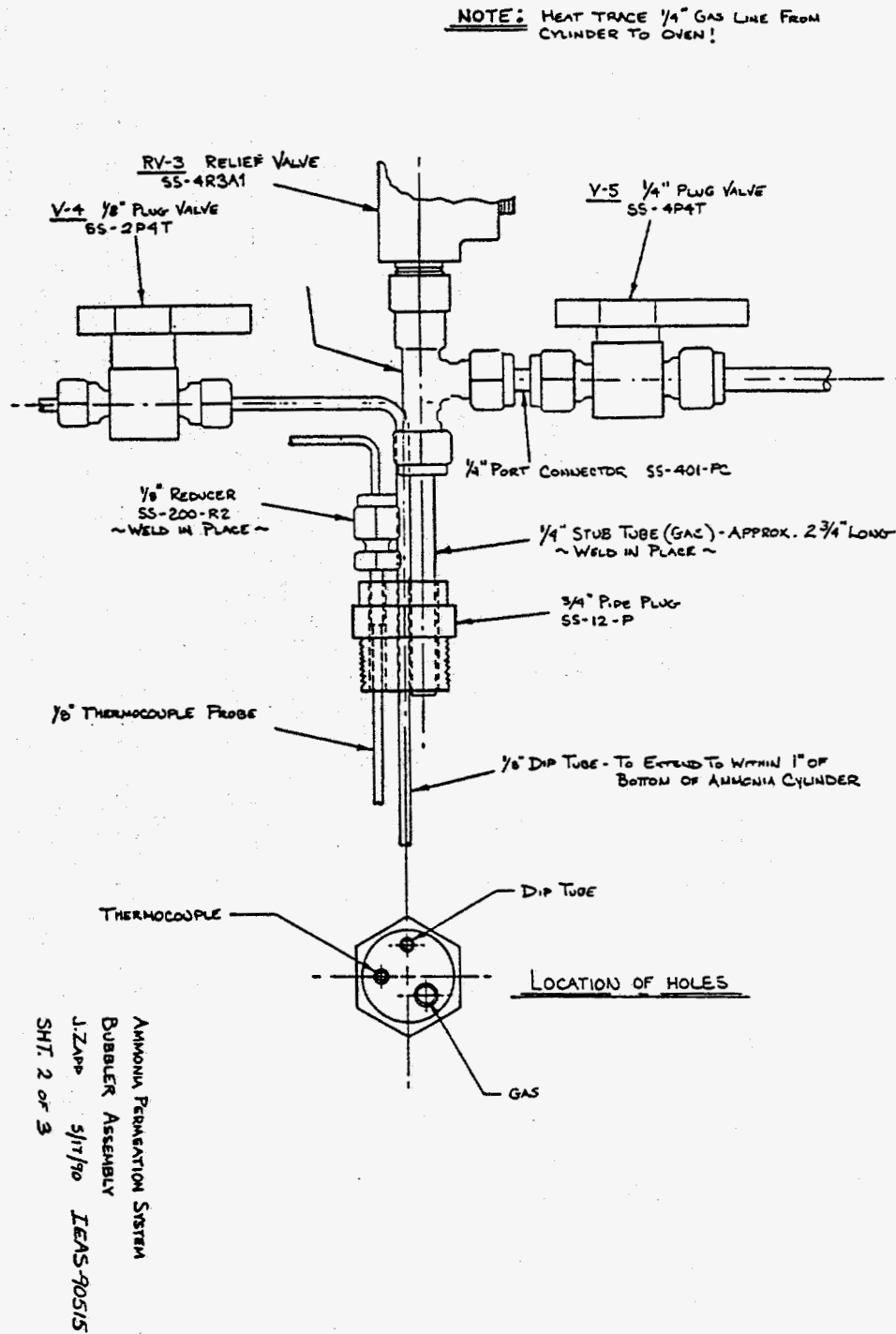


Figure 4.2-2: CYL-2 Connection Assembly -Expanded View

Figure 2.3-5: High Pressure Membrane Test System

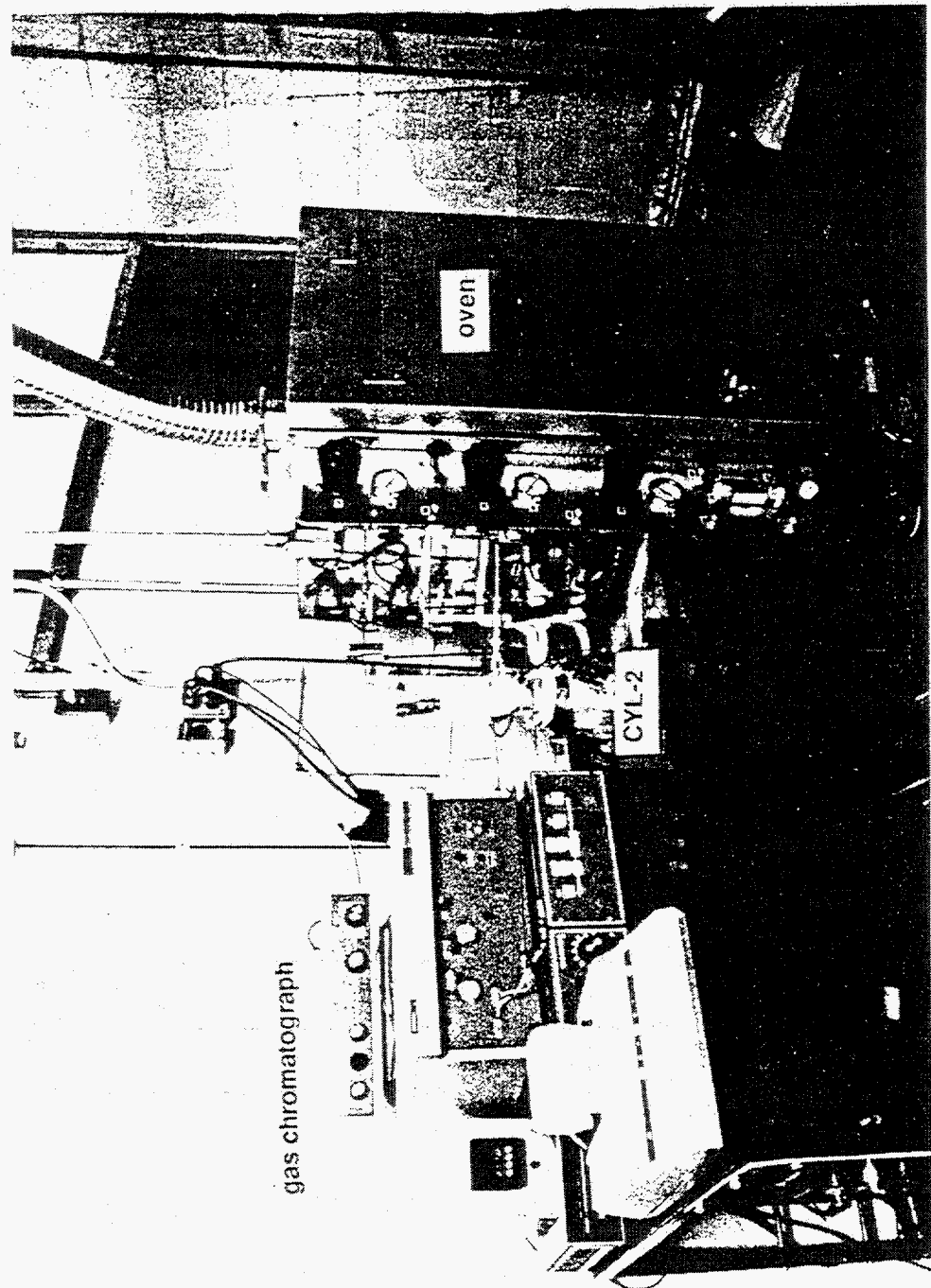


Figure 4.2-3: High Pressure Membrane Test Unit

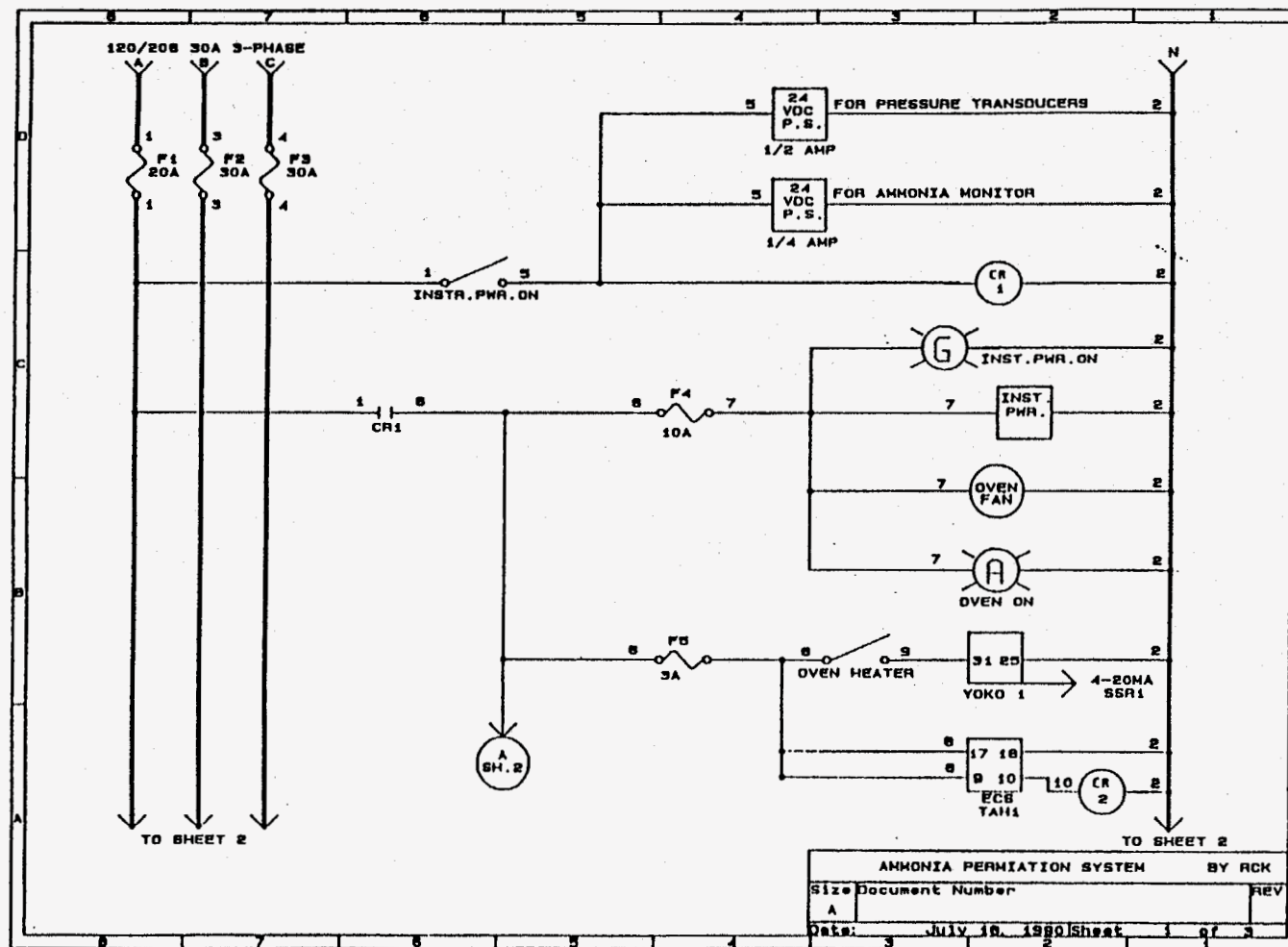


Figure 4.2-4: Electrical Wiring Diagram - High Pressure Membrane Test System

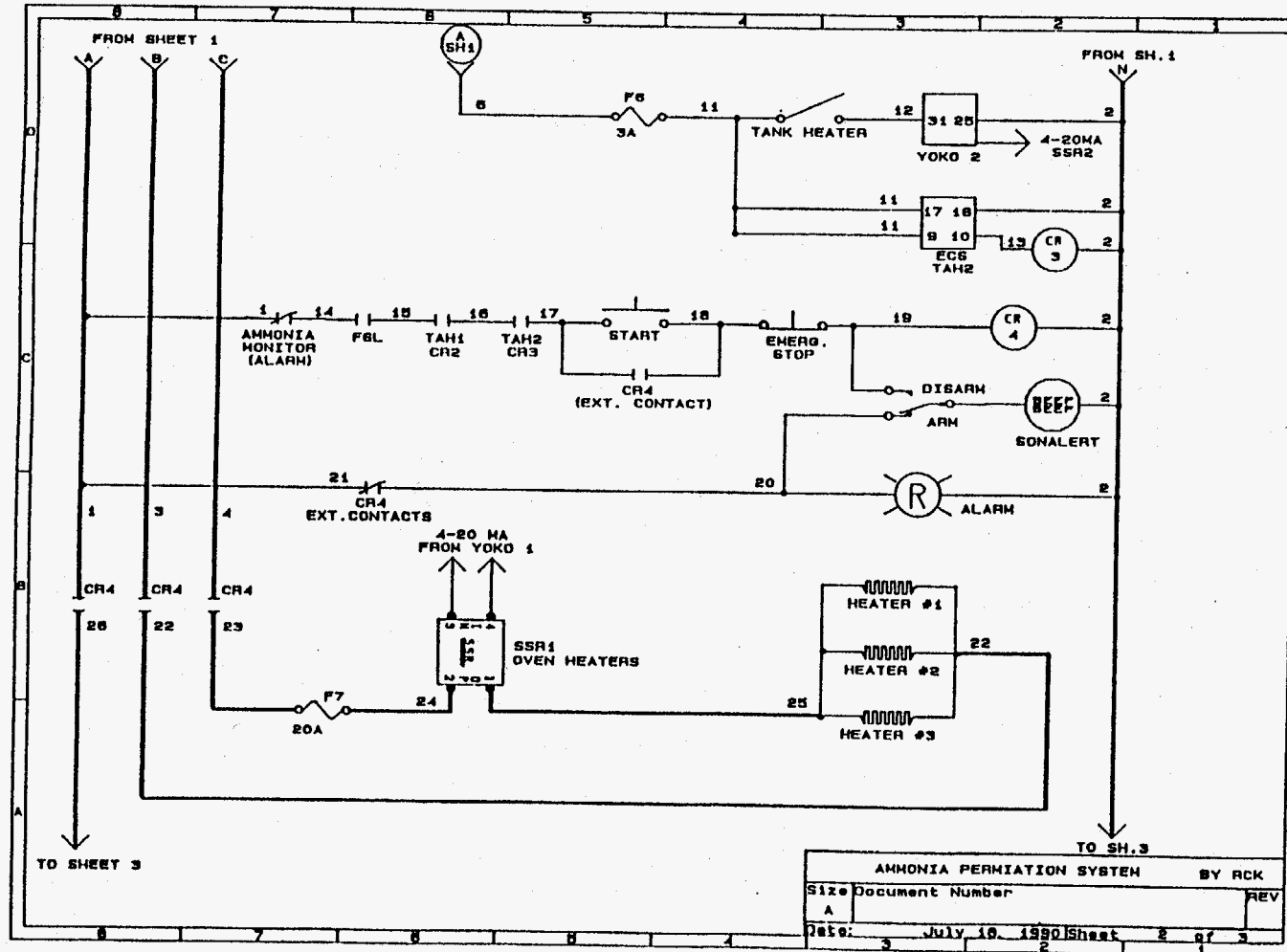


Figure 4.2-4: Electrical Wiring Diagram - High Pressure Membrane Test System (cont)

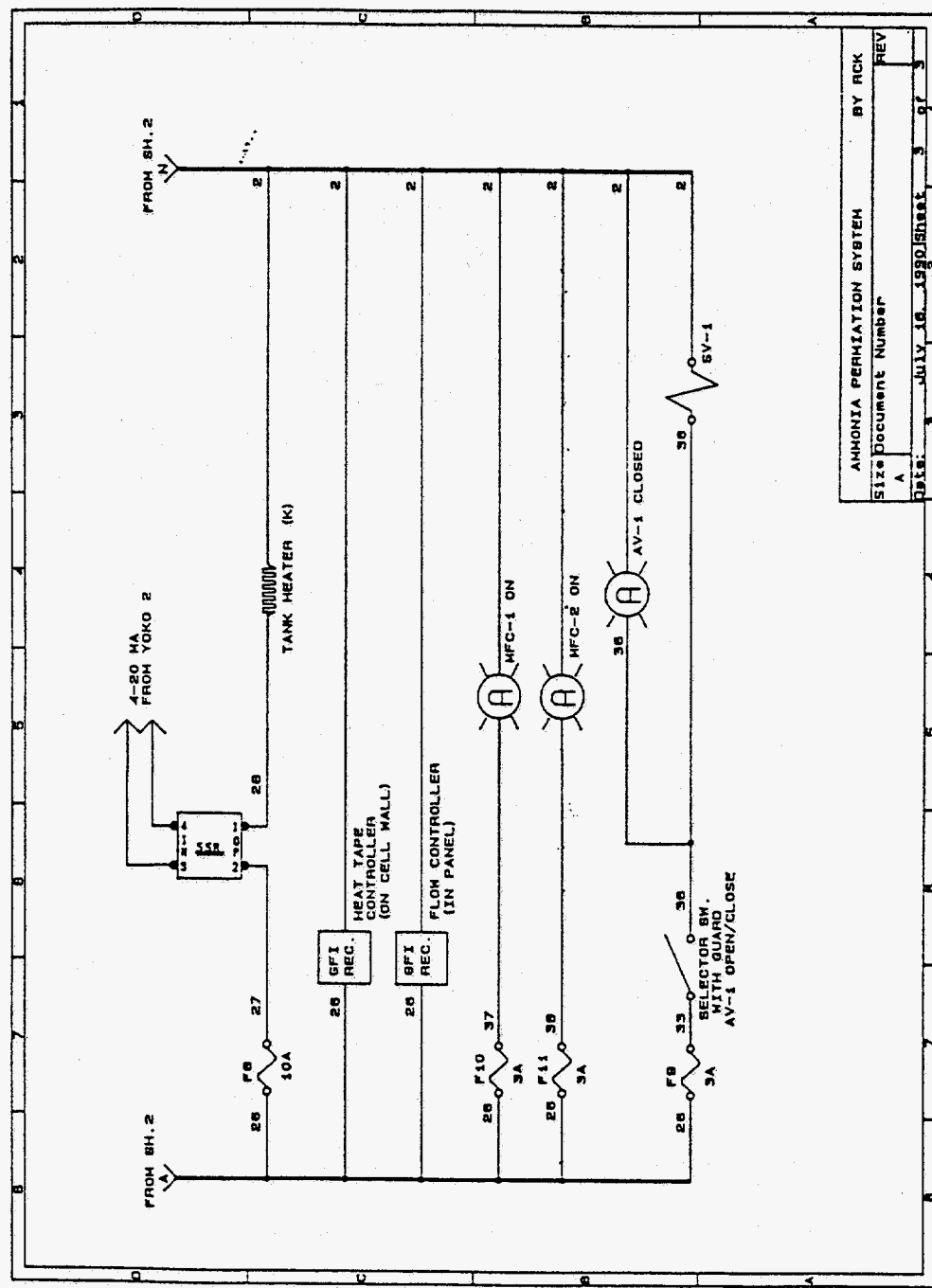


Figure 4.24: Electrical Wiring Diagram - High Pressure Membrane Test System (cont)

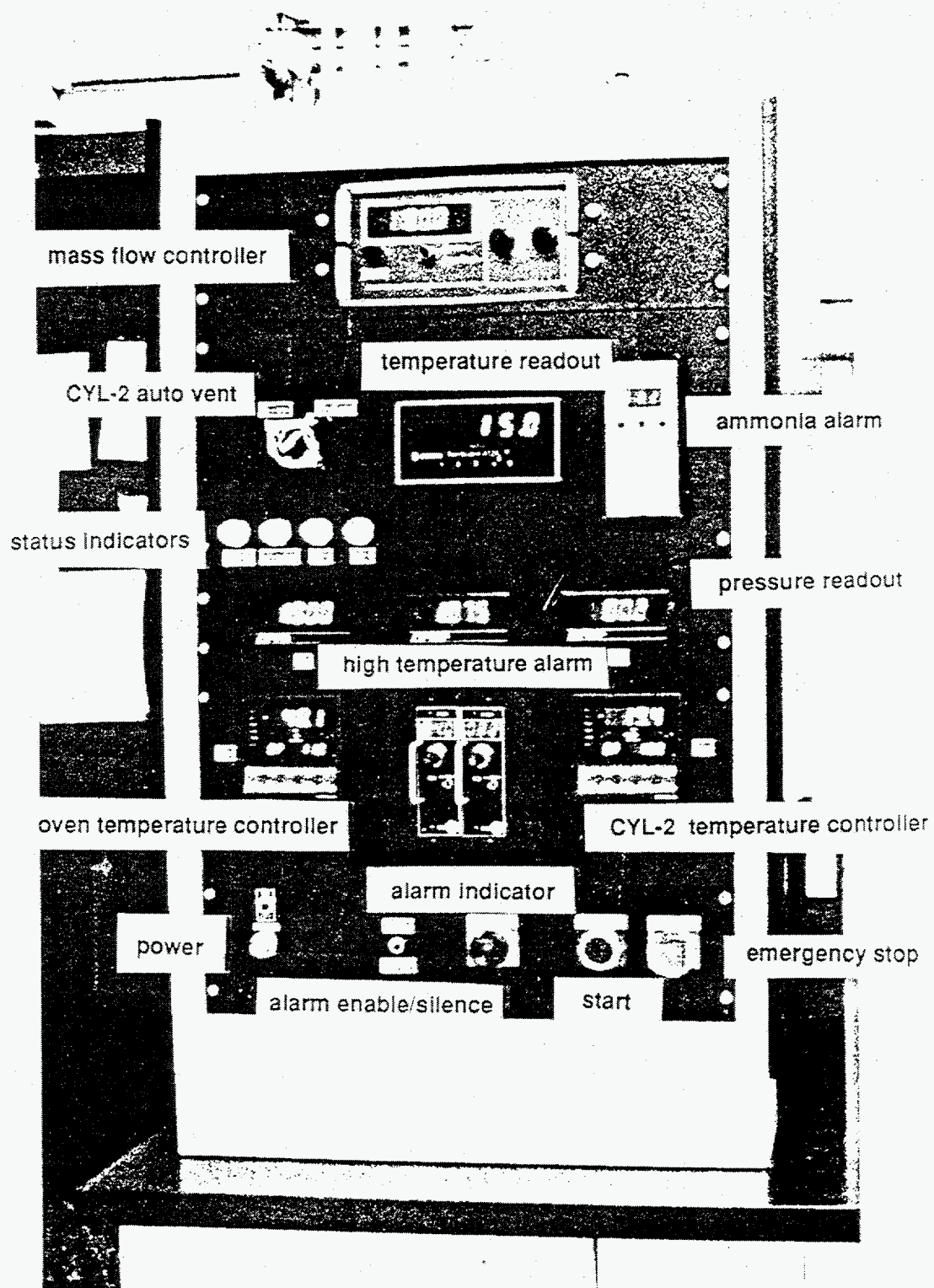


Figure 4.2-5: Control Cabinet - High Pressure Membrane Test Unit

4.2.3 Component List

PCV-1	15-2000 psig pressure regulator
PCV-2	0-250 psig pressure regulator
PCV-3	0-50 psig pressure regulator
BPR-1,2	200-2500 psig backpressure regulator
BPR-3	0-250 psig backpressure regulator
MFC-1,2	0-500 sccm high pressure, mass flow controller
AV-1	air actuated valve
FI-1	tube type flow meter
SV-1	solenoid valve
EFV-1	excess flow valve 1slm
V1-2	shut-off valve
V3-V6	plug valve
V7-V10	sample valve
V-11,12	needle valve
CV-1-CV-4	check valve, 10psi
RV-1	relief valve, 3000 psia
RV-2	relief valve, 300 psia
RV-3	relief valve, 2200 psia
RV-4	relief valve, 50 psia
HTR-1	Neslab chiller/heater unit
TIC-1,2	temperature controller
CYL-2	"D" size steel cylinder, modified
TIC-3	heat tape controller
PT-3	pressure transducer, 1000 psia
PT-1,2	pressure transducer, 2000 psia
PI's	process signal conditioner/power supply
TI-2	temperature indicator
TAH1,2	high temperature alarm
PI-3,4	pressure gauge, 2000 psia
PI-5	pressure gauge, 300 psia

4.2.4 Conversion to CO₂ Applications

The high pressure test unit can be converted from NH₃ to CO₂ application testing by performing the following operations:

- 1) CYL-2 is filled with H₂O rather than NH₃
- 2) CYL-1 is replaced by a blend of CH₄ in H₂
- 3) MFC-1 is recalibrated for the new CH₄/H₂ blend
- 4) GC columns are replaced with CO₂ compatible columns (e.g., Poropak)

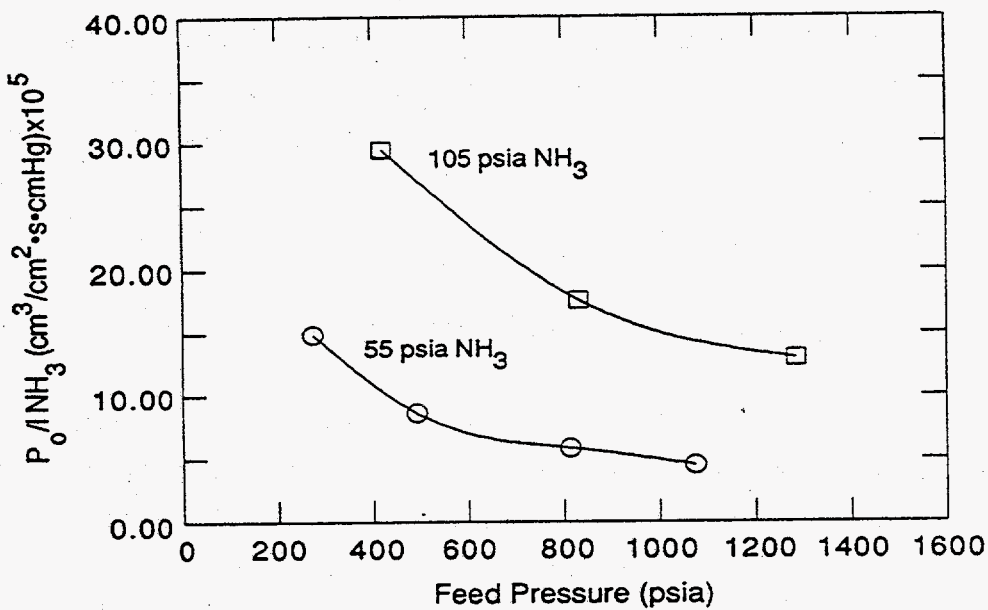
4.3 Evaluation of NH₃-Selective MLC Membranes

The membranes tested in this part of the program were MLCs of the type PTMSP/PVAmSCN/PTMSP or PTMSP/PVAmSCN/PAN/Hollytex. The latter is typical of a composite which would be used in an actual commercial module. Fabrication of such MLC membranes is detailed in ref. 8. In the process of evaluating the composite membranes, a number of experimental parameters are set, e.g., feed flow rate, pressures and partial pressures, temperatures etc. In the following sections only those parameters relevant to the discussion at hand are given. Full experimental details and complete results are given in Appendix A.

4.3.1 Evaluation of NH₃-selective MLCs as a Function of Feed Gas Pressure

These experiments were designed to 1) test the mechanical stability of the membrane as the total transmembrane pressure (the difference in total pressure between the feed and permeate sides of the membrane) was increased to pressures greater than 1000 psia, and 2) track the permselectivity of the membrane under these conditions. To perform these measurements experimentally, the NH₃ bubbler temperature was chosen to yield an NH₃ partial pressure representative of one of the points in the test matrix. The remainder of the feed gas pressure consisted of gas from the cylinder containing N₂/ H₂ (CYL-1). For each set of experiments, the NH₃ partial pressure in the feed stream was held constant and only the pressure of N₂ and H₂ was increased. In this way it was possible to test the dimensional stability of the membrane at increasingly harsher conditions. For these tests the membranes were PTMSP/PVAmSCN/PAN/Hollytex MLCs. Results are summarized in Figure 4.3-1. Details of the experimental parameters and complete results are given in Appendix A.

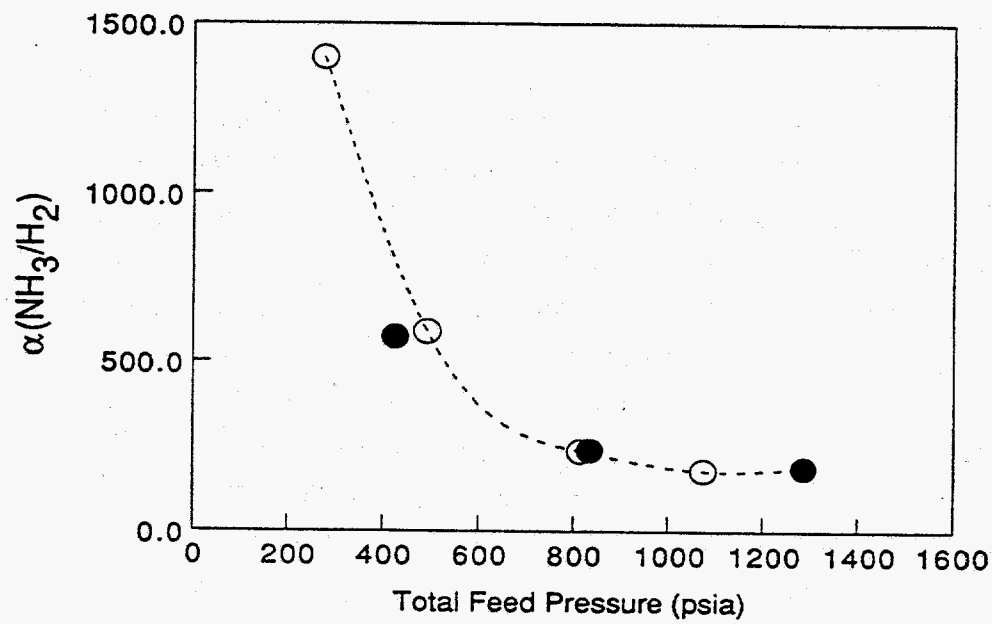
Figure 4.3-1
Evaluation of MLC Membrane as a Function of Feed Pressure



11497-36, 11497-92; $T_{mem} = 40^\circ C$

The membrane is able to withstand transmembrane pressure gradients in excess of 1000 psi. To our knowledge, this is the first time that a facilitated transport membrane has been operated successfully at these high pressures. To have demonstrated dimensional stability at these pressures represents a milestone in the program. Somewhat surprising is the fact that as the feed pressure is increased, the observed flux of NH₃ (Po/l) decreases. This is unexpected since the NH₃ partial pressure in the feed and permeate gases, and hence the driving force for NH₃ permeation, is constant; one would expect a constant Po/l NH₃ as the system pressure is increased. This is apparently not the case and, if true, has two important implications. First, the obvious feature that the membrane is less productive at high pressures. The NH₃ flux at 1200 psia is only 25% of the flux at 300 psia. Second, since the flux (Po/l) of N₂ and H₂ is essentially constant for the pressure range studied (Appendix A), $\alpha(NH_3/N_2)$ and $\alpha(NH_3/H_2)$ decrease with increasing total pressure simply as a result of the loss of NH₃ flux (Figure 4.3-2). For instance, at 55 psia NH₃, and 275 psia total feed pressure $\alpha(NH_3/H_2)$ is 1400 but at 1075 psia $\alpha(NH_3/H_2)$ is only 180. Thus, at the low pressure condition the observed Po/l NH₃ and

Figure 4.3-2
NH₃/H₂ Selectivity of PTMSP/PVAmSCN/PAN/HT MLC Membrane



11497-36,92; $T_{\text{mem}}=40^{\circ}\text{C}$

selectivities are near the target values of 40 and 1500, respectively (see Table 4.1-2) but fall short at pressures under which the membrane would eventually be used in a commercial application. It is therefore important to understand if the observed loss in NH₃ flux, and consequently in selectivity, is real or an artifact of the experiment.

4.3.2 Role of PAN Support Layer

One possible explanation of the phenomenon centers on physical changes in the MLC brought about by the high pressure test. Specifically, the integrity of the asymmetric microporous support polymer (e.g., the poly(acrylonitrile)) after it is subjected to a large pressure drop. To investigate this possibility, we examined cross-sections of the MLC before and after permeation testing. The photomicrographs, shown in Figure 4.3-3, reveal a significant change in the macroporous region of the PAN layer. The highly oriented macropores have essentially collapsed and now form a tortuous, less porous path. To further investigate the role of the PAN macropore region, we repeated the previous permeation measurements but this time used a membrane which did not contain an asymmetric support layer. If the PAN layer contributes significantly to the flux loss, then we would expect to see significantly less flux loss in the membranes fabricated without this layer. Results are shown in Figure 4.3-4.



PAN

PVAmSCN PTMSP

PVAmSCN PAN

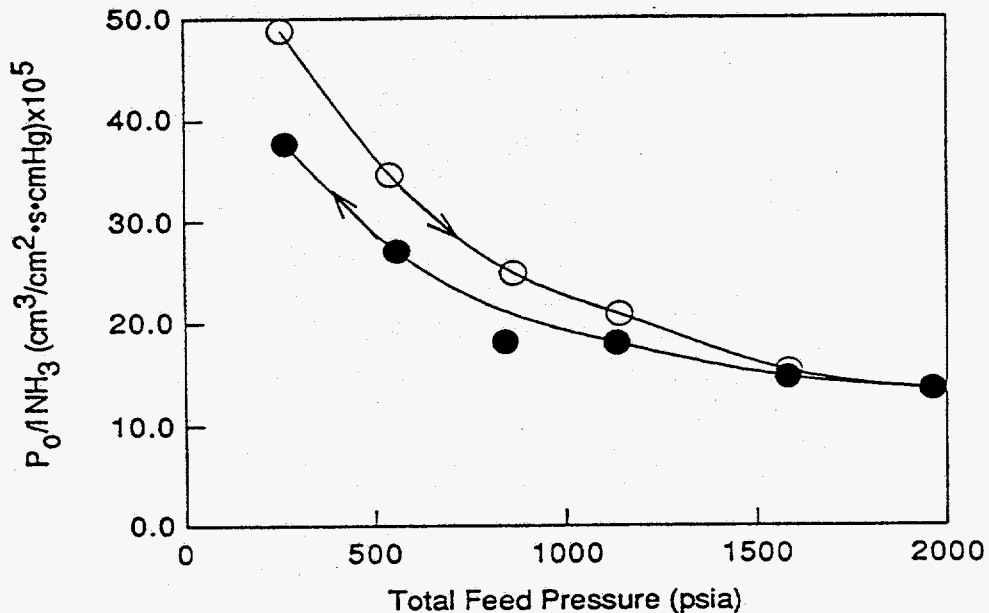
Before

After Testing at 2000 psi



Figure 4.3.3: Scanning Electron Micrographs of MLC Before and After Permeation Testing (11497-73)

Figure 4.3-4
Evaluation of PTMSP/PVAmSCN/PTMSP MLC Membrane



11497-73; $P_{NH_3}=55$ psia; $T_{mem}=40^\circ C$

Although the absolute value of the NH_3 flux is higher for this membrane than the previous membranes, the loss in flux is essentially the same. This data indicates that the loss of macroporosity in the PAN layer accompanying high pressure testing is not significantly limiting mass transfer across the membrane. The fact that the membrane without the PAN/Hollytex support possesses higher flux values of all gases simply indicates that the PAN layer imposes some mass transfer resistance to permeation due to its low surface microporosity.

4.3.3 Concentration Polarization

Another source of the flux loss revolves around a phenomenon known as "concentration polarization." Concentration polarization is observed most often in membranes which are both highly permeable and highly selective, e.g., RO, UF and pervaporation membranes, but generally not gas separation, since those membranes typically have low selectivity. The phenomenon is associated with the formation of a boundary layer at the feed/membrane interface

under steady-state conditions (Figure 4.3-5). The boundary layer forms because the region near the membrane surface is depleted of the faster permeating gas (in our case NH₃). A new gas phase mass transfer barrier is established through which NH₃ from the bulk composition must diffuse before reaching the membrane surface. As the pressure is increased, the mass transfer resistance of this boundary layer increases owing to the additional partial pressure of the nonpermeating gases. In short, there is poor mixing in the space directly over the membrane.

As one might expect, the extent of concentration polarization is dependent on the mixing patterns in the test cell/module and consequently the geometry of the test. If the loss in flux arises from poor mixing, then improving the mixing (e.g. by increasing the flow rate of feed gas) would be expected to restore some of the flux loss. Results from such experiments, in which the NH₃ permeance was measured at different pressures as a function of feed gas flow rate, are shown in Figure 4.3-6. As is evident, increasing the feed flow rate has a marked effect on the observed P₀/1 NH₃. At low total pressures (\approx 250 psi) only a small (but significant) increase in observed NH₃ flux is realized. Indeed, at low pressures there is no difference between the flux measured at a feed gas flow rate of 250 sccm and 450 sccm. We believe this value represents the membrane-limited NH₃ flux. The effect of feed flow rate becomes more pronounced as the total pressure is increased. At high pressure, nearly 75% of the flux loss has been restored. Other data, given in Appendix A, provide additional support for these conclusions (see e.g., 11478-92).

F4.3-5

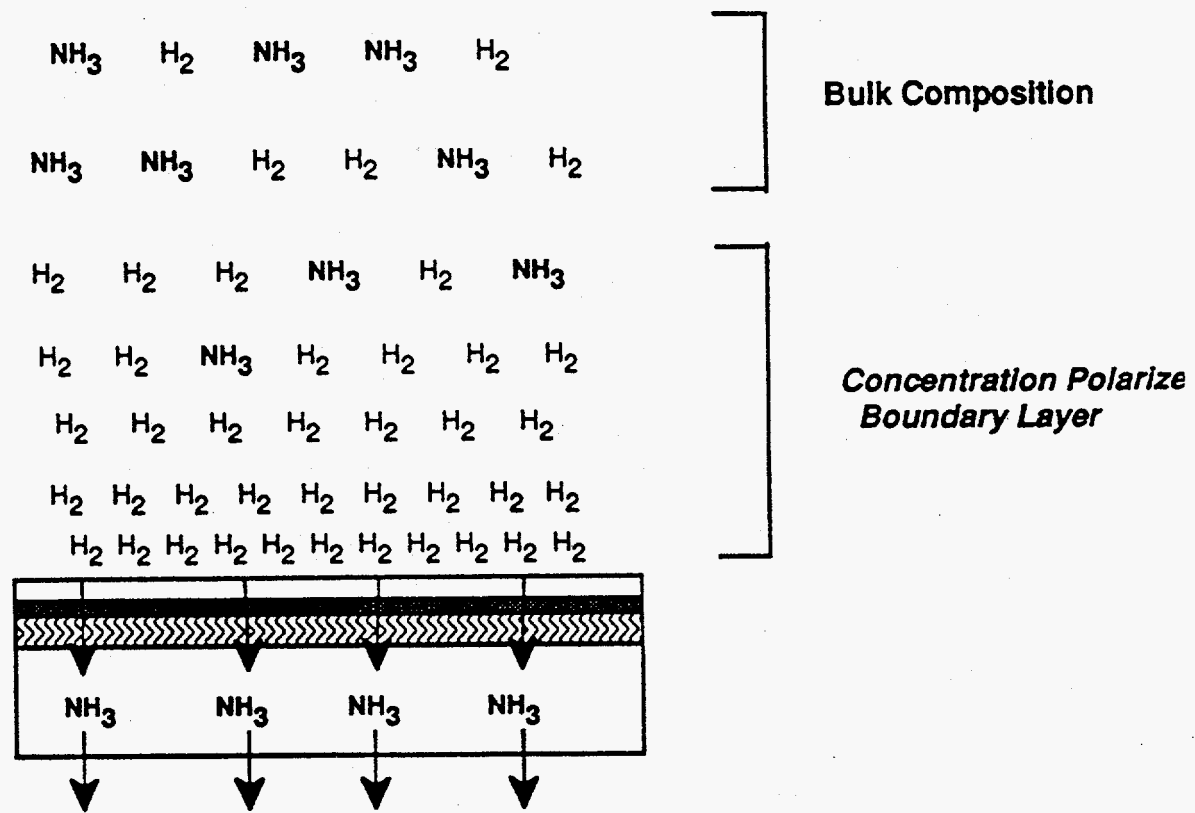
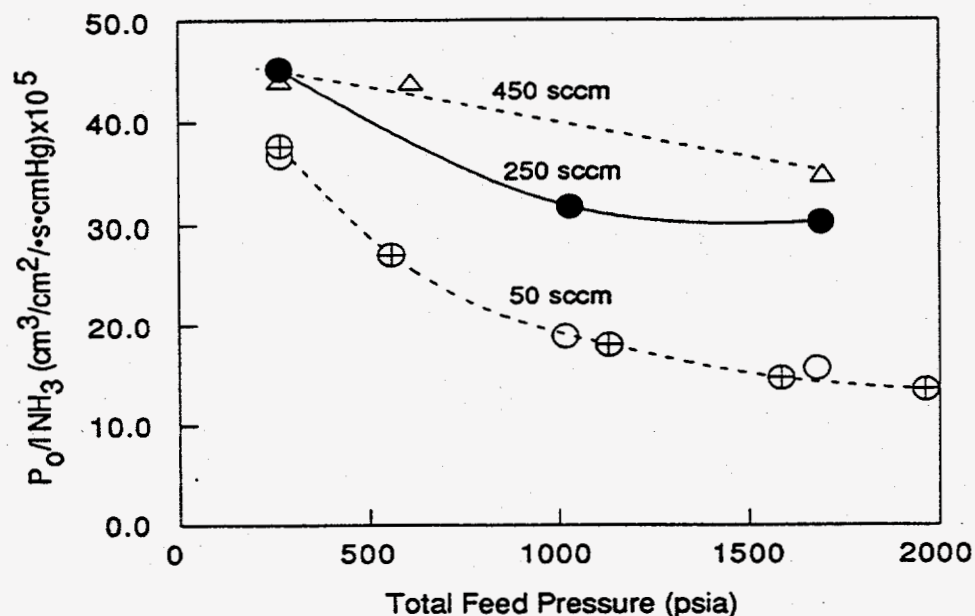


Figure 4.3-5: Concentration Polarization Phenomenon

Figure 4.3-6
Effect of Feed Flow Rate on Membrane Performance
(PTMSP/PVAmSCN/PTMSP)



11497-73; $P_{NH_3} = 55$ psia; $T_{mem} = 40^\circ C$

This explanation can be verified by a simple calculation of the mass transfer coefficient of a boundary layer using estimates of the NH_3 diffusion coefficient in the $H_2/N_2/NH_3$ mixture. Table 4.3-1 lists the diffusion coefficients for the indicated conditions as calculated by CAPP, an APCI computer-based thermodynamics program. As expected, the diffusivity is almost exactly inversely proportional to pressure. The flux loss displayed in Figure 4.3-4 could be explained if there were a mass transfer resistance proportional to total pressure and having a mass transfer coefficient of about 38×10^{-5} scc/cm²·s·cmHg at 1000 psia. This resistance is in series with the resistance of the membrane itself. A simple scenario which can lead to such a resistance is that of a stagnant layer above the membrane surface through which the ammonia must diffuse. The resistance of such a layer is given by

$$r = D_m/dRT$$

where D_m = diffusion coefficient, cm^2/s

d = thickness of the stagnant layer, cm

T = temperature, K

R = gas constant ($0.2784 \text{ cm}^3 \cdot \text{cmHg}/\text{scc} \cdot \text{K}$)

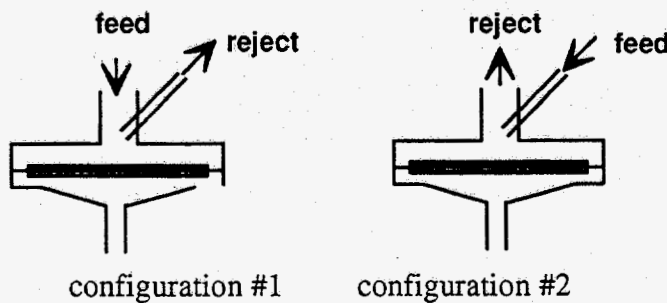
Mass transfer is a potential explanation of the results in Figure 4.3-4 if the layer thickness, d , is less than the approximately 1 cm distance between the membrane surface and the outlet tube.

Inserting the values of $r = 38 \times 10^{-5} \text{ scc}/\text{cm}^2 \cdot \text{s} \cdot \text{cmHg}$, $D_m = 0.0056 \text{ cm}^2/\text{s}$ and $T = 313\text{K}$ gives $d = 0.17 \text{ cm}$. This is small enough to conclude that mass transfer is a potential explanation for the observed results.

Table 4.3-1
Diffusion Coefficients for Ammonia

Pressure, psia	250	500	1000	2000
Temperature, C	40	40	40	40
Gas Composition				
NH ₃ , %	22	11.0	5.5	2.75
N ₂ , %	46.8	53.4	56.7	58.35
H ₂ , %	31.2	35.6	37.8	38.90
NH ₃ Diffusivity:				
ft ² /hr	0.0832	0.0421	0.0215	0.0112
cm ² /s	0.0215	0.0109	0.0056	0.0028

To further test this theory we examined the effect of reversing the direction of the feed input and feed reject gas flows. This was possible to do because the test cell is highly unsymmetrical as shown below.



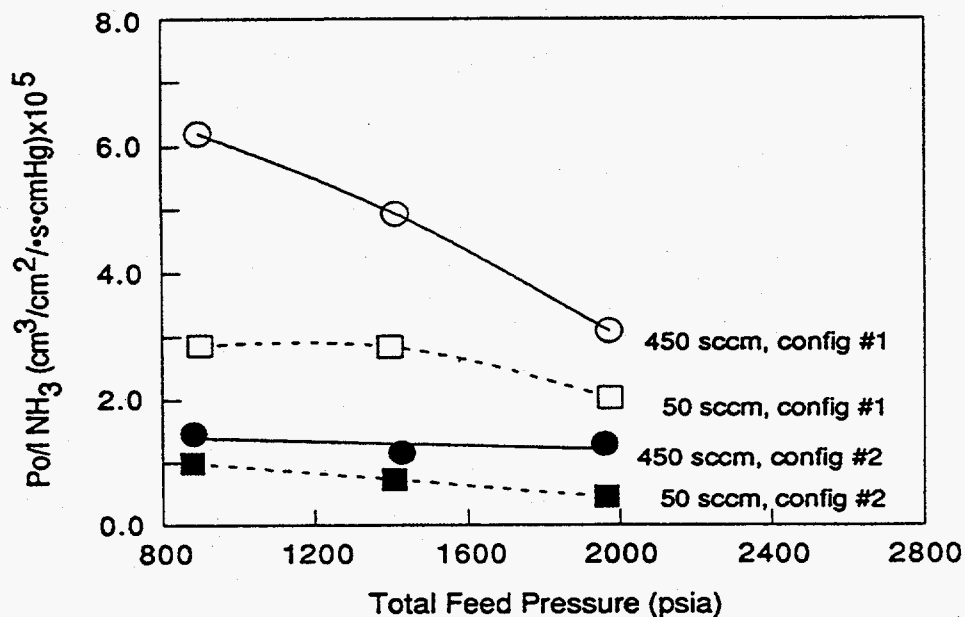
In configuration #1, the standard configuration used for all previous tests, the feed gas enters directly above the membrane through a 3/8" diameter orifice and exits at an angle ($\sim 45^\circ$) to the membrane surface through a 1/8" diameter tube. In configuration #2 the feed gas enters through the smaller orifice and exits through the larger. If concentration polarization plays a dominant role then one would expect a significant difference in the measured NH_3 flux for the two configurations. Results are shown in Figure 4.3-7. In configuration #1 we observe the typical NH_3 flux loss as the total feed gas pressure is increased. In configuration #2 the decrease in NH_3 flux with total feed pressure is not significant, however the NH_3 flux for both flow rates is considerably lower than in configuration #1. This is strong evidence for the concentration polarization effect.

4.3.4 Evaluation of MLC Membranes at Process Conditions

This section summarizes results for a variety of membranes which were tested under "process conditions". It was experimentally difficult to obtain precisely those conditions outlined in the test plan, but every attempt was made to set experimental parameters which would be useful in evaluating the utility of these membranes. Results are summarized in Table 4.3-1.

The MLC membranes were able to withstand the high transmembrane pressures for all test conditions. This is especially important for cases in which the NH_3 partial pressure in the feed gas is quite high, and consequently, the membrane contains large quantities of sorbed NH_3 ; that is, the "active transport" layer is highly gelled under these conditions. In general, as the driving force (difference in NH_3 partial pressure between feed and permeate interfaces) is decreased the NH_3 permeance decreases. This is also an indication of polarization induced mass transfer limitations. As expected, permeance is a strong function of temperature due to the equilibrium between gas phase NH_3 and NH_3 sorbed in the membrane.

Figure 4.3-7
Effect of Test Cell Geometry on Membrane Performance
(PTMSP/PVAmSCN/PAN/HT)



11786-63B, $T_{mem}=60^{\circ}\text{C}$, $P_{\text{NH}_3}=55$ psia

Table 4.3-2
Evaluation of MLC Membranes at Process Conditions

membrane	T (°C)	P _{tot} (psia)	P _{NH₃} (psia)	P _{derm} (psia)	Po/I NH ₃ * (cm ³ /cm ² ·s·cmHg) × 10 ⁵	α(NH ₃ /H ₂)	α(NH ₃ /N ₂)
11497-44	65	1928	55	53	6.9	449	696
11497-44	65	1938	145	55	2.9	76	250
11786-1	40	1984	105	19	8.8	127	379
11786-15	40	1973	105	44	10.2	251	689
11786-40	40	1998	125	42	16.1	777	4984
11786-40	60	1967	240	69	16.6	238	1000
11786-55	60	1710	125	68	2.9	69	346
11786-59	60	1695	240	105	0.5	14	26

In reviewing this data, one should bear in mind that it was collected before the concentration effects were fully appreciated. Therefore, one must be careful not to infer too much about the usefulness of these membranes (from an economic point of view) from this data. The results should be appreciated for what they actually indicate; that is, that the membranes are stable at elevated temperatures and extreme transmembrane pressures and exhibit reasonable permselectivity.

4.3.5 Lifetime of MLC Membranes

On-stream data for membranes tested in task 2 is summarized in the table below. Most membranes survived testing intact. In general, testing was terminated for reasons other than membrane failure, e.g., cooling bath failure, scheduled equipment or facilities maintenance. On-stream membrane evaluation represents 20 weeks of task 2 activities.

<u>Membrane Run #</u>	<u>Time on Stream (days)</u>	<u>Comments</u>
11497-36	7	ok
11497-44	19	ok but tore upon depressurization
11497-73	23	ok, exp. terminated to refill NH ₃ supply
11497-92	8	formed a hole
11497-101	9	ok
11786-1	14	ok, some discoloration
11786-15	9	cooling bath failure
11786-40	15	ok
11786-55	8	ok
11786-59B	8	ok
11786-63B	16	ok

Total= 136 hrs (19.5 weeks)

4.4 Summary/Status

PTMSP/PVAmSCN/PAN/HT Multilayer Composite Membranes have been shown to be stable at the very high transmembrane pressures required by the process applications (NH₃ synthesis plant). Feed gas flow rate and test cell orientation strongly effect the observed NH₃ permeance and NH₃/H₂ and NH₃/N₂ selectivity of these membranes. These results indicate that concentration polarization plays a predominant role in limiting mass transfer of NH₃ through these membranes at high feed pressures. This issue will need to be addressed in downstream fabrication of modules.

While membranes have been evaluated per the membrane test plan, some deviations were necessary to investigate the observed loss in NH₃ flux (concentration polarization). Thus the last point in the test matrix was not completed. It will not be necessary to complete the test matrix before proceeding to task 3 (see section 5.3, planning).

5.0 Conclusions and Recommendations

5.1 Microencapsulation

Air Products' "Active Transport" materials have been microencapsulated within a shell of the gas permeable polymer poly(trimethylsilylpropyne). Gas absorption studies demonstrate that the capsules selectively absorb NH₃ and CO₂ from gas streams and could, in principle, be used to perform a pressure- or temperature-swing absorption-based separation of these gases from mixtures with e.g., N₂, H₂ or CH₄. For example, PTMSP-encapsulated NH₄SCN had an NH₃/N₂ selectivity of 185 at 25°C, and PTMSP-encapsulated TEAA•4H₂O had a CO₂/N₂ selectivity of 43 at 50°C. The selectivity will increase if higher payloads can be achieved. Most of the capsules fabricated were 100-500 µm in diameter - larger than the target 25-50 µm needed to fabricate practical gas separation membranes. Two runs produced capsules 30-50 µm in diameter, however, they could not be harvested before they agglomerated into larger particles.

Recommendation:

No further experimental work is planned under this cooperative agreement. Air Products is actively pursuing patent protection on the fabrication and use of microencapsulated liquid absorbents for gas separation.

5.2 MLC Membranes

The multilayer composite (MLC) technique is viable for fabricating membranes which utilize Air Products' proprietary AT CO₂-selective materials. Carbon dioxide permeance of 0.2×10^{-5} cm³/cm²•s•cmHg and CO₂/H₂ selectivity of 80 were observed for laboratory flat sheet membranes. A 10-fold decrease in AT layer thickness is required for these membranes to compete effectively with alternate CO₂ removal technologies. The MLC design was proven to be stable for up to 3 weeks of continuous operation.

Recommendation:

Air Products recommends further testing of CO₂-selective MLCs under end-use conditions. This work will be done in part under the cooperative agreement and in part under an Air Products'-funded materials development program. Air Products further recommends that fabrication of lab-scale membrane modules proceed on schedule as outlined in section 5.3.

Ammonia-selective MLC membranes were fabricated and evaluated under end-use conditions. The MLC design is able to withstand the high transmembrane pressure (2000 psi) required in Air Products' membrane-based process for recovering NH₃ from the ammonia synthesis process. Concentration polarization effects were observed in membranes tested under high pressure. These effects should be considered in future module designs. The MLC membranes were demonstrated to be stable for up to 3 weeks of continuous operation.

Recommendation:

Air Products recommends that fabrication of lab-scale membrane modules proceed on schedule as outlined in section 5.3.

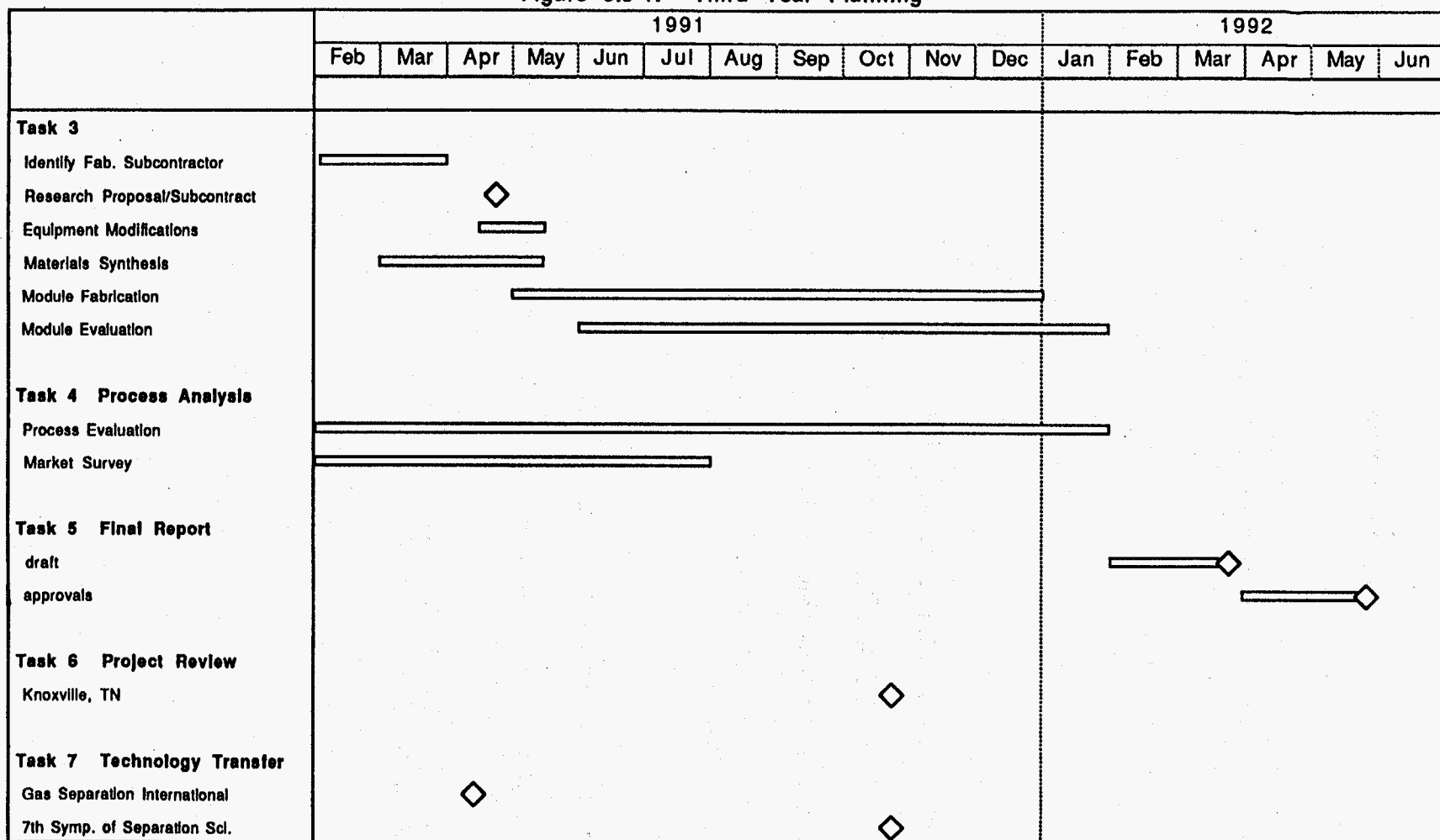
5.3 Third Year Planning

Based on promising results from the first and second budget periods we recommend the following action plan for the third budget period of this cooperative agreement.

- 1) Synthesize sufficient quantities of Air Products AT materials to fabricate lab-scale membrane modules. We estimate approximately 500 g each of PTMSP, PVAmSCN, PDMS and DADMAF will be needed for work during the third budget year.
- 2) Modify membrane test equipment to accommodate lab-scale modules (e.g. changeout mass flow controller valves, increase scrubber capacity etc)
- 3) Identify and contract with a suitable fabrication partner to fabricate lab-scale spiral wound modules.
- 4) Measure permselectivity and lifetimes of lab-scale membrane modules under process conditions.

Task planning for the third budget period of this program is shown in Figure 5.3-1.

Figure 5.3-1: Third Year Planning



6.0 References

1. Air Products and Chemicals, Inc., Technical Proposal to the United States Department of Energy, Office of Industrial Programs for "Development of Novel Active-Transport Membrane Devices," September 1987, p. 42.
2. D. V. Laciak, "Development of Novel Active Transport Membrane Devices," Interim Report, February 1990, p. 117.
3. Ibid., p. 149.
4. Ibid., p.119.
5. M. Langsam et al., Gas Separation and Purification, 2, (1988), p. 162.
6. S.T. Hwang et al., Sep.Sci. and Tech. 9, (1979), p. 461.
7. Hayaishi et al., U.S. Pat. No. 4384017 (1983).
8. D. V. Laciak, "Development of Novel Active-Transport Membrane Devices," Interim Report, February 1990, p. 61.
9. Ibid., p.135.
10. D. W. Brubaker and K. Kammermeyer, Ind.Ind.Chem., 46, (1954), p. 733.
11. D. V. Laciak, "Development of Novel Active Transport Membrane Devices," Interim Report, February 1990, p. 63.
12. R. Quinn, D. V. Laciak et al, "Polyelectrolyte Membranes for the Separation of Acid Gases," U.S. Pat. No. 5,336,298 (1994)

7.0 Appendix

Summary of NH₃-Selective MLC Test Runs

This Appendix contains the experimental parameters used during the evaluation of NH₃-selective MLC membranes. It also contains the detailed results from each test. The material is arranged in spreadsheet form by membrane number.

1497-36

8

	A	B	C	D	E	F	G	H	I	J	K	L	M	N	O	P
41																
42																
43	Lab Book #		11497-44	cont												
44	Date		8/22/90	Rev:3/12/91												
45																
46	NH3 Temp (°C)		0.0													
47	Oven Temp (°C)		65.0													
48	Trace Temp (°C)		60.0													
49																
50	Mem Area (cm ²)		0.8													
51	Feed N2/H2		0.32													
52	P(NH3) feed (psia)		55													
53	Sweep Rate (sccm)		10.0													
54																
55	Total Pressure (psia)	Total Pressure (cmHg)	N2 Pressure (cmHg)	H2 Pressure (cmHg)	Flow Rate (sccm)		Pressure (psia)	%NH3	%N2	%H2	Total Comp	Po/l NH3x105	Po/l N2x105	Po/l H2x105	NH3/N2	NH3/H2
57																
58	1929.00	9993.46	3180.31	6758.15	115.0		15.00	0.50	0.24	0.73	7.47	8.66	0.016	0.023	422.55	293.97
59	1931.00	10003.82	3183.62	6765.20	125.0		15.00	0.25	0.24	0.73	7.22	8.38	0.016	0.023	404.98	281.75
60	1930.00	9998.64	3181.96	6761.67	115.0		15.00	0.00	0.23	0.71	6.94	8.11	0.015	0.022	404.28	277.17

1	A	B	C	D	E	F	G	H	I	J	K	L	M	N	O	P
2																
3	Lap Book #		11497-44-2	44 00M												
4	Date		8/23/90	860V:3/12/91												
5	NH3 Temp (C)		0.0													
6	Over Temp (C)		65.0													
7	Trace Temp (C)		60.0													
8	Mem Area (nm2)		0.8													
9	Feed N2/H2		0.32													
10	Speed Feed (psia)		55													
11	Speed Feed (pscm)		5.0													
12	P(NH3) feed (psia)															
13	Speed Feed (pscm)															
14																
15																
16																
17	Total Pressure (psia)															
18	Total Pressure (psia)															
19	182.00	9998.20	3178.65	6754.03	115.0	53.00	5.25	0.31	1.20	6.76	8.05	0.010	0.019	786.88	426.71	
20	182.00	9998.20	3178.65	6754.03	115.0	53.00	5.25	0.31	1.20	6.76	8.05	0.010	0.019	786.88	426.71	440.77

	A	B	C	D	E	F	G	H	I	J	K	L	M	N	O	P
40																
41																
42																
43	Lab Book #		11497-44-2	cont												
44	Date		8/24/90	Rev:3/12/91												
45	NH3 Temp (°C)		25.0													
46	Oven Temp (°C)		65.0													
47	Trace Temp (°C)		60.0													
48																
49	Mem Area (cm ²)		0.6													
50	Feed N2/H2		0.32													
51	P(NH3) feed (psia)		145													
52	Sweep Rate (scm)		5.0													
53																
54																
55	Total Pressure (psia)	Total Pressure (cmHg)	N2 Pressure (cmHg)	H2 Pressure (cmHg)	Flow Rate (scm)		Pressure (psia)	% NH3	% N2	% H2	Total Comp	Vol NH3x105	Vol N2x105	Vol H2x105	NH3/N2	NH3/H2
56	1905.00	9869.12	3111.72	6612.40	225.0		55.00	8.00	0.41	2.68	11.09	1.66	0.014	0.043	120.05	38.25
57	1938.00	10040.08	3186.43	6728.66	200.0		55.00	12.60	0.35	2.40	15.35	2.90	0.012	0.038	250.73	76.23
58	316.00	1637.08	477.47	1014.82	200.0		49.00	46.00	15.00	37.00	98.00	14.04	4.191	6.493	3.35	2.16

	A	B	C	D	E	F	G	H	I	J	K	L	M	N	O	P	
41																	
42																	
43	Lab Book #		11497-73														
44	Date		12/5/90	Rev:3/12/91													
45																	
46	NH3 Temp (°C)		0.0														
47	Oven Temp (°C)		40.0														
48	Trace Temp (°C)		23.0														
49																	
50	Mem Area (cm ²)		0.8														
51	Feed N2/H2		0.32														
52	P(NH3) feed (psia)		55														
53	Sweep Rate (sccm)		10.0														
54																	
55																	
56	Total Pressure (psia)		Total Pressure (cmHg)	N2 Pressure (cmHg)	H2 Pressure (cmHg)	Flow Rate (sccm)		Pressure (psia)	%NH3	%N2	%H2	Total Comp	Po/l NH3x105	Po/l N2x105	Po/l H2x105	NH3/N2	NH3/H2
57																	
58	1678.00	6693.12	2704.20	5873.92	50.0			15.00	14.75	0.50	5.70	20.95	15.66	0.038	0.215	413.12	72.83
59	1690.00	8755.28	2784.09	5916.19	250.0			15.00	24.25	0.45	4.40	29.10	30.29	0.034	0.162	895.12	186.79
60	1695.00	8781.19	2792.38	5933.61	450.0			15.00	27.00	0.50	5.00	32.50	34.97	0.038	0.185	932.22	189.09
61		0.00	-17.60	-37.40									0.00	#NUM!	#NUM!	#NUM!	#NUM!

	A	B	C	D	E	F	G	H	I	J	K	L	M	N	O	P
1																
2																
3																
4																
5																
6																
7																
8																
9																
10																
11																
12																
13																
14																
15																
16																
17																
18																
19																
20																
21																
22																
23																
24																

	A	B	C	D	E	F	G	H	I	J	K	L	M	N	O	P
1																
2																
3	Lab Book #	11497-101														
4	Date	12/5/90	Rev:3/12/01													
5																
6	NH3 Temp (°C)	15.0														
7	Oven Temp (°C)	40.0														
8	Trace Temp (°C)	42.0														
9																
10	Mem Area (cm ²)	0.8														
11	Feed N2/H2	0.38														
12	P(NH3) feed (psia)	105														
13	Sweep Rate (cccm)	10.0														
14																
15																
16	Total Pressure (psia)	Total Pressure (cmHg)	N2 Pressure (cmHg)	H2 Pressure (cmHg)	Flow Rate (cccm)	Pressure (psia)	% NH3	% N2	% H2	Total Comp	Ps/l NH3x105	Ps/l N2x105	Ps/l H2x105	NH3/N2	NH3/H2	
17																
18	417.00	2160.33	781.02	1274.30	50.0	15.00	32.75	0.00	0.07	32.82	21.75	0.000	0.011	#DIV/0!	1699.12	
19	426.00	2208.95	798.74	1303.21	450.0	15.00	35.75	0.00	0.06	35.03	24.85	0.000	0.013	#DIV/0!	1941.49	
20	826.00	4279.21	1586.20	2588.01	50.0	15.00	18.25	0.00	0.24	18.49	9.95	0.000	0.019	#DIV/0!	513.75	
21	830.00	4299.93	1594.07	2600.86	450.0	15.00	19.25	0.00	0.27	19.52	10.63	0.000	0.022	#DIV/0!	489.85	
22	1241.00	6429.18	2403.19	3920.99	50.0	15.00	14.00	0.00	0.31	14.31	7.25	0.000	0.017	#DIV/0!	430.47	
23	1220.00	6320.38	2391.85	3853.54	450.0	15.00	15.25	0.00	0.34	15.59	8.01	0.000	0.018	#DIV/0!	434.15	

A	B	C	D	E	F	G	H	I	J	K	L	M	N	O	P				
1																			
2																			
3	Lab Book #	11786-1																	
4	Date	12/5/90	Rev:3/12/91																
5																			
6	NH3 Temp (°C)	15.0																	
7	Oven Temp (°C)	40.0																	
8	Trace Temp (°C)	42.0																	
9																			
10	Mem Area (cm ²)	0.8																	
11	Feed N2/H2	0.36																	
12	P(NH3) feed (psia)	105																	
13	Sweep Rate (sccm)	10.0																	
14																			
15	Total Pressure (psia)	Total Pressure (cmHg)	N2 Pressure (cmHg)	H2 Pressure (cmHg)	Flow Rate (sccm)		Pressure (psia)	% NH3	% N2	% H2	Total Comp	Pa/l	NH3x105	Pa/l	N2x105	Pa/l	H2x105	NH3/N2	NH3/H2
16																			
17																			
18	1163.00	6025.09	2249.63	3670.45	50.0		22.00	27.50	0.09	1.00	28.59	18.19	0.008	0.057	2180.60	318.96			
19	1128.00	5843.78	2180.73	3556.03	50.0		18.00	20.25	0.13	0.93	21.31	11.62	0.012	0.055	933.95	211.11			
20	1141.00	5911.11	2206.32	3599.79	450.0		20.00	25.25	0.13	1.24	26.82	15.79	0.012	0.073	1284.34	217.01			
21	1640.00	8498.25	3188.68	5202.58	50.0		18.00	16.00	0.17	1.19	17.38	8.66	0.011	0.048	778.49	179.43			
22	1645.00	8522.15	3198.52	5218.64	450.0		21.00	21.25	0.19	1.58	23.02	12.67	0.012	0.064	1021.94	197.49			
23	1980.00	10154.06	3818.64	6230.41	50.0		18.00	10.75	0.44	1.73	12.92	5.28	0.024	0.059	218.94	89.56			
24	1984.00	10278.39	3865.89	6307.50	450.0		19.00	16.25	0.43	2.08	10.74	6.81	0.023	0.070	378.51	126.86			
25	1981.00	10159.24	3820.61	6233.63	50.0		46.00	7.75	0.44	1.47	9.86	4.98	0.024	0.050	205.29	98.92			
26	1985.00	10283.57	3867.86	6310.71	450.0		46.00	10.50	0.48	2.07	13.05	7.11	0.026	0.070	272.94	101.22			

	A	B	C	D	E	F	G	H	I	J	K	L	M	N	O	P
1																
2																
3	Lab Book #		11786-15													
4	Date		12/17/90	Rev:3/12/91												
5																
6																
7	NH3 Temp (°C)		15.0													
8	Oven Temp (°C)		40.0													
9	Trace Temp (°C)		42.0													
10	Mem Area (cm ²)		0.8													
11	Feed N2/H2		0.32													
12	P(NH3) feed (psia)		105													
13	Sweep Rate (sccm)		10.0													
14																
15																
16	Total Pressure (psia)	Total Pressure (cmHg)	N ₂ Pressure (cmHg)	H ₂ Pressure (cmHg)	Flow Rate (sccm)		Pressure (psia)	%NH3	%N ₂	%H ₂	Total Comp	Po/l NH3x105	Po/l N ₂ x105	Po/l H ₂ x105	NH3/N ₂	NH3/H ₂
17																
18	1988.00	10195.50	3228.96	6861.54	50.0		16.00	12.50	0.17	0.63	13.50	6.37	0.011	0.025	579.59	250.49
19	1696.00	6786.37	2778.04	5903.33	450.0		18.00	19.25	0.19	1.42	20.86	10.85	0.014	0.031	759.51	213.13
20	1950.00	10102.25	3199.12	6798.13	50.0		42.00	10.50	0.21	0.92	11.63	7.03	0.014	0.029	512.56	246.53
21	1973.00	10221.40	3237.25	6879.15	450.0		44.00	14.25	0.23	1.32	15.80	10.23	0.015	0.041	688.93	251.86
22	1940.00	10050.44	3182.54	6782.90	50.0		40.00	11.25	0.23	0.68	12.16	7.50	0.015	0.021	498.19	354.85

A	B	C	D	E	F	G	H	I	J	K	L	M	N	O	P
40															
41															
42															
43	Lab Book #	11786-40	cont												
44	Date	1/21/91	Rev:3/12/01												
45															
46	NH3 Temp (°C)	42.0													
47	Oven Temp (°C)	60.0													
48	Trace Temp (°C)	58.0													
49															
50	Mem Area (cm ²)	0.1													
51	Feed N2/H2	0.38													
52	P(NH3) feed (psia)	240													
53	Sweep Rate (sccm)	5.0													
54															
55															
56	Total Pressure (psia)	Total Pressure (cmHg)	N2 Pressure (cmHg)	H2 Pressure (cmHg)	Flow Rate (sccm)	Pressure (psia)	% NH3	% N2	% H2	Total Comp	Po/I NH3x105	Po/I N2x105	Po/I H2x105	NH3/N2	NH3/H2
57															
58	1985.00	10179.98	3777.18	6162.77	50.0	31.00	10.50	0.00	0.39	10.89	11.23	0.000	0.066	#DIV/0!	169.65
59	1947.00	10086.71	3741.75	6104.98	50.0	27.00	9.25	0.00	0.33	9.58	9.58	0.000	0.056	#DIV/0!	169.58
60	1974.00	10226.58	3794.90	6191.68	450.0	32.00	48.00	0.07	1.93	50.00	88.69	0.019	0.331	4612.10	267.85
61	1972.00	10216.22	3790.96	6185.26	450.0	52.00	34.25	0.10	0.92	35.27	55.27	0.027	0.156	2071.31	353.44
62	1973.00	10221.40	3792.93	6188.47	50.0	43.00	0.00	0.00	0.00	#NUM!	#NUM!	#NUM!	#NUM!	#NUM!	
63	1985.00	10283.57	3818.56	6227.01	450.0	55.00	22.25	0.12	0.64	23.01	30.80	0.033	0.108	938.92	205.65
64	1971.00	10211.04	3789.00	6182.05	450.0	71.00	12.00	0.06	0.32	12.38	16.02	0.017	0.054	970.00	298.11
65	1967.00	10190.32	3781.12	6169.20	450.0	69.00	12.50	0.06	0.41	12.97	16.56	0.017	0.070	1000.55	238.16
66	1730.00	8962.51	3314.55	5407.98	450.0	40.00	29.25	0.09	0.78	30.12	41.33	0.026	0.151	1459.47	272.91
67	1720.00	8910.70	3294.87	5375.84	450.0	17.00	41.25	0.05	1.01	42.31	63.19	0.016	0.198	3995.18	319.60
68	1703.00	8822.63	3261.40	5321.23	450.0	54.00	0.00	0.00	0.00	#NUM!	#NUM!	#NUM!	#NUM!	#NUM!	
69	1731.00	8967.09	3316.52	5411.17	450.0	17.00	29.25	0.00	0.81	30.06	37.20	0.000	0.157	#DIV/0!	238.64

	A	B	C	D	E	F	G	H	I	J	K	L	M	N	O	P
1																
2																
3		Lab Book #	11786-55													
4		Date	1/29/91													
5																
6		NH3 Temp (°C)	20.0													
7		Oven Temp (°C)	60.0													
8		Trace Temp (°C)	84.0													
9																
10		Mem Area (cm ²)	0.8													
11		Feed N2/H2	0.36													
12		P(NH3) feed (psia)	125													
13		Sweep Rate (sccm)	5.0													
14																
15																
16	Total Pressure (psia)	Total Pressure (cmHg)	N2 Pressure (cmHg)	H2 Pressure (cmHg)	Flow Rate (sccm)		Pressure (psia)	% NH3	% N2	% H2	Total Comp	Po/I NH3x105	Po/I N2x105	Po/I H2x105	NH3/N2	NH3/H2
17																
18	1720.00	8910.70	3162.85	5622.85	450.0		18.00	28.00	0.23	3.98	32.21	7.15	0.008	0.077	941.61	92.93
19	1710.00	8858.90	3144.20	5589.89	450.0		68.00	9.25	0.25	2.17	11.67	2.88	0.008	0.042	346.32	68.82

	A	B	C	D	E	F	G	H	I	J	K	L	M	N	O	P			
41																			
42																			
43	Lab Book #	11786-55																	
44	Date	12/1/91																	
45																			
46	NH3 Temp (°C)	-13.5																	
47	Oven Temp (°C)	60.0																	
48	Trace Temp (°C)	58.0																	
49																			
50	Mem Area (cm ²)	0.8																	
51	Feed N2/H2	0.36																	
52	P(NH3) feed (psia)	35																	
53	Sweep Rate (sccm)	5.0																	
54																			
55																			
56	Total Pressure (psia)	Total Pressure (cmHg)	N2 Pressure (cmHg)	H2 Pressure (cmHg)	Flow Rate (sccm)		Pressure (psia)	% NH3	% N2	% H2	Total Comp	Po/I	NH3x105	Po/I	N2x105	Po/I	H2x105	NH3/N2	NH3/H2
57																			
58	1686.00	8734.56	3131.84	5567.72	450.0		44.00	0.75	0.31	0.50	1.56	1.10	0.010	0.009	104.56	116.70			
59	1689.00	8750.10	3137.44	5577.67	450.0		44.00	1.00	0.25	0.70	1.95	1.63	0.008	0.013	194.44	124.02			

A	B	C	D	E	F	G	H	I	J	K	L	M	N	O	P	
1																
2																
3	Lab Book #	11786-638	(11478-68-2)													
4	Date	2/28/91														
5																
6	NH3 Temp (°C)	0.0														
7	Oven Temp (°C)	60.0														
8	Trace Temp (°C)	64.0														
9																
10	Mem Area (cm ²)	0.8														
11	Feed N2/H2	0.84														
12	P(NH3) feed (psia)	55														
13	Sweep Rate (sccm)	5.0														
14																
15																
16	Total Pressure (psia)	Total Pressure (cmHg)	N2 Pressure (cmHg)	H2 Pressure (cmHg)	Flow Rate (sccm)		Pressure (psia)	% NH3	% N2	% H2	Total Comp	Po/I NH3x105	Po/I N2x105	Po/I H2x105	NH3/N2	NH3/H2
17	original															
18	885.00	4584.87	2699.11	1630.75	450.0		20.00	25.50	0.00	0.33	25.03	19.52	0.000	0.024	#DIV/0!	824.08
19	1413.00	7320.25	4649.76	2615.49	450.0		20.00	22.25	0.15	0.53	22.93	16.17	0.003	0.023	4801.13	714.19
20	1917.00	9831.29	6320.82	3555.48	450.0		19.00	19.75	0.19	0.75	20.69	13.42	0.003	0.023	4278.56	579.44
21	reverse											0.00				
22	1399.00	7247.72	4603.34	2589.38	450.0		20.00	9.50	0.22	0.58	10.30	5.77	0.005	0.024	1155.86	237.70
23	879.00	4553.78	2878.22	1619.56	450.0		20.00	10.25	0.22	0.37	10.64	6.36	0.008	0.025	796.71	251.51
24	0.00	-35.20	-19.80								0.00					
25	906.00	4693.66	2968.74	1669.92	450.0		20.00	11.25	0.18	0.38	11.81	7.09	0.006	0.025	1119.31	280.85
26	original										0.00					
27	898.00	4652.22	2942.22	1655.00	450.0		20.00	10.00	0.22	0.34	10.56	6.20	0.008	0.023	792.76	273.13
28	1398.00	7242.54	4600.02	2587.51	50.0		18.00	5.25	0.27	0.42	5.94	2.85	0.006	0.017	464.22	164.17
29	1411.00	7309.88	4643.13	2611.76	450.0		20.00	8.25	0.26	0.45	8.96	4.94	0.006	0.019	844.08	265.98
30	1975.00	10231.77	6513.13	3663.64	50.0		20.00	3.75	0.28	0.52	4.55	2.03	0.004	0.015	452.09	135.23
31	1973.00	10221.40	6508.50	3659.91	450.0		20.00	5.50	0.30	0.58	6.38	3.10	0.005	0.016	843.38	190.55
32	reverse										0.00					
33	1985.00	10179.96	6479.87	3644.99	50.0		18.00	1.00	0.35	0.36	1.71	0.46	0.006	0.010	80.64	43.99
34	1980.00	10154.06	6463.40	3635.66	450.0		20.00	2.50	0.33	0.46	3.29	1.30	0.005	0.013	242.20	98.94
35	1408.00	7294.34	4633.18	2606.18	50.0		19.00	1.50	0.30	0.32	2.12	0.74	0.007	0.013	108.56	56.93
36	1427.00	7392.77	4698.18	2641.80	450.0		20.00	2.25	0.30	0.34	2.89	1.17	0.007	0.014	175.41	86.30
37	878	4548.80	2875.91	1617.70	50.0		18.00	2.00	0.31	0.26	2.57	1.00	0.011	0.017	88.58	58.66
38	882	4569.33	2889.17	1625.16	450.0		20.00	2.75	0.30	0.32	3.37	1.47	0.011	0.021	135.03	70.00
39	original				0.0		0.00	0.00	0.00	0.00	0.00	#NUM!	#VALUE!	#VALUE!	#NUM!	

98